Ph.D. Dissertation of Medicine

RNA-seq transcriptomic profiling of manually microdissected kidney

- Biomarker study of glomerulonephritis -

미세분리기법을 활용한 신장 조직 전사체 프로파일링 연구

February 2023

Graduate School of Medicine
Seoul National University
Biomedical Sciences Major

Sehoon Park

RNA-seq transcriptomic profiling of manually microdissected kidney

- Biomarker study of glomerulonephritis -

Yon Su Kim

Submitting a Ph.D. Dissertation of
Medicine

October 2022

Graduate School of Medicine
Seoul National University
Biomedical Sciences Major

Sehoon Park

Confirming the Ph.D. Dissertation written by
Sehoon Park
January 2023

Chair _____(Seal)
Vice Chair _____(Seal)
Examiner _____(Seal)
Examiner _____(Seal)
Examiner _____(Seal)

Abstract

RNA-seq transcriptomic profiling of manually microdissected kidney

- Biomarker study of glomerulonephritis -

Sehoon Park
Biomedical Sciences Major
The Graduate School
Seoul National University

Transcriptome profiling of microdissected kidney substructure can reveal pathophysiologic changes specific to glomerulus and tubulointerstitial tissue. The author aimed to perform RNA-seq analysis of manually microdissected kidney biopsy tissues in this study. The study included major glomerulonephritis patients to study disease specific or a biomarker with uniform changes in diverse glomerulonephritis. Considering that IgAN is one of the most common primary glomerulonephritis worldwide with clinical importance, the author profiled the glomerulus transcriptomic profile of the disease category to investigate a IgAN-related transcript signature. In addition, as tubulointerstitial fibrosis is the common final pathways of various glomerulonephritis, the author profiled the tubule-transcriptome of glomerulonephritis.

In glomerulus RNA-seq, the author collected glomeruli from biopsy specimens from IgAN patients with relatively preserved kidney function (eGFR ≥ 60 mL/min/1.73 m^2 and urine protein-to-creatinine ratio < 3 g/g) and from normal kidney cortices by manual microdissection and performed RNA-seq. Differentially expressed

genes (DEG) were identified, and gene-ontology term annotation and pathway analysis were performed. Immunohistochemical labeling and primary mesangial cell cultures were performed to confirm the findings of RNA-seq analysis. Total of 14 IgAN patients and 10 controls were included in this glomerulus RNA-seq. Glomerulus-specific genes were highly abundant. Principal component analysis showed clear separation between the IgAN and control groups. There were 2,497 DEGs, of which 1,380 were upregulated and 1,117 were downregulated (false discovery rate < 0.01). The enriched gene ontology terms included motility/migration, protein/vesicle transport, and immune system, and the kinase binding was the molecular function overrepresented in IgAN. B cell signaling, chemokine signal transduction, and FcγR-mediated phagocytosis were the canonical pathways overrepresented. *In vitro* studies confirmed that spleen tyrosine kinase (SYK), reported as upregulated in the IgAN transcriptome, was also upregulated in the glomeruli from an independent set of IgAN patients and that treatment with patient-derived IgA1 increased the expression of SYK in mesangial cells.

In tubulointerstitial RNA-seq, the author profiled manually microdissected tubulointerstitial tissue from biopsy cores of 65 glomerulonephritis cases, including 43 patients with IgAN, 3 with diabetes mellitus nephropathy, 3 with focal segmental glomerulosclerosis, 3 with lupus nephritis, 4 with membranous nephropathy, and 9 with minimal change disease, and additional 22 nephrectomy controls by RNA sequencing. A potential biomarker was selected based on the false discovery rate, and experiments were performed in TNF-α-stimulated primary cultured human tubular epithelial cells (hTECs). The author identified 3037 genes with low expression and 2852 genes with high expression in the disease

samples compared to the controls. Dual-specificity phosphatase 1 (DUSP1) exhibited universal low expression in various diseases (log2 fold change, -3.87), with the lowest false discovery rate (7.03E-132). In further experimental validation study, DUSP1 overexpression ameliorated inflammatory markers related with MAP kinase pathways in hTECs, while pharmacologic inhibition of DUSP1 increased these markers. The combination of DUSP1 overexpression with low-concentration corticosteroid treatment resulted in more potent suppression of inflammation than high-concentration corticosteroid treatment alone.

In conclusion, transcriptome profiling of glomerulus and tubulointerstitial tissue in patients with various glomerulonephritis revealed notable findings that may provide insights into pathophysiologic mechanisms. Future studies may consider the clinical implementation of the identified biomarkers and test whether the modification of the targets may be helpful in treatment of glomerulonephritis.

Keyword : Kidney, glomerulonephritis, transcriptomics, genomics

Student Number : 2016-21982

Table of Contents

Chapter 1. Introduction

1.1. Study Background

Glomerulonephritis is one of the major etiologies of chronic kidney disease.[1] Both primary glomerulonephritis, such as immunoglobulin A nephropathy (IgAN) and secondary nephropathies, such as diabetic kidney disease, are related to kidney function decline, and major health problems affecting patient problem and causing substantial socioeconomic burden.

Kidney is a complex organ consisting of diverse microstructure. Not only the functions of microstructures are various but also the pathophysiologic mechanism may be different in the pathologic structures (e.g. glomerulus, tubulointerstitial tissue). Therefore, investigation for the pathophysiologic changes in the specific structures may enhance the understandings of the underlying mechanisms of glomerulonephritis. Microdissection is a technique to isolate kidney substructures manually and has been a useful tool to investigate the pathophysiologic changes specific to glomerulus or tubulointerstitium.

Transcriptomic profiling provides the opportunity of

unsupervised investigation for the abundance of messenger RNA expression. In particular, high-throughput RNA sequencing (RNA-seq) overcomes the previous limitations of microarray techniques, enabling a transcriptome annotation with clearer resolution.[2,3] Several RNA-seq investigations for the transcriptomic profiling of glomerulonephritis have been performed, yet, a study including diverse kidney disease categories was rare particularly implementing the microdissection technique to reveal the microstructure-specific kidney transcriptomic profiles.

1.2. Purpose of research

In this study, the author aimed to perform transcriptomic profiling of manually microdissected kidney biopsy tissues.[3,4] The study included major glomerulonephritis patients to study disease specific or a biomarker with uniform changes in diverse glomerulonephritis. Considering that IgAN is one of the most common primary glomerulonephritis worldwide with clinical importance, the author profiled the glomerulus transcriptomic profile of the disease category to investigate a

IgAN-related transcript signature. In addition, as tubulointerstitial fibrosis is the common final pathways of various glomerulonephritis, the author profiled the tubule-transcriptome of glomerulonephritis. The author performed additional experimental validation to determine whether the identified transcriptomic profiles compared to nephrectomy tissue controls may suggest a clinically relevant biomarker.

Chapter 2. Methods

2.1. Ethical Considerations

The institutional review boards of Seoul National University Hospital approved this study and the usage of biospecimens from the National Biobank of Korea (No. H-1706-139-816). The National Biobank of Korea obtained the kidney biopsy samples with the informed consent of the patients. The study was performed in accordance with the principles of the Declaration of Helsinki.

2.2. Procurement of kidney tissue samples

Biopsy cores from glomerulonephritis patients were obtained from punch biopsies performed between 2010 and 2017 and stored in RNAlater (Qiagen, Hamburg, Germany) at -80°C.[3]

For glomerulus transcriptomic profiling, the author selected 16 IgAN samples with relatively preserved kidney function, as they had estimated glomerular filtration rate (eGFR) > 60 mL/min/1.73 m2 and random urine protein-to-creatinine ratio <

3 g/g at the time of kidney biopsy. Total of 10 control samples for glomerulus RNA-seq were obtained from the non-cancerous cortical tissue of the kidney that was removed for the treatment of renal cell carcinoma. The control subjects had no evidence of underlying kidney dysfunction or other medical conditions such as diabetes mellitus or hypertension. These nephrectomy control group samples were also stored in RNAlater immediately after surgical excision via the same protocol used for the biopsy core tissues.

For transcriptomic profiling for tubulointerstitial tissue, the author collected samples from 46 patients with IgAN, 3 with diabetes mellitus nephropathy, 3 with focal segmental glomerulosclerosis, 3 with lupus nephritis, 4 with membranous nephropathy, and 9 with minimal change disease. Similar as the samples included in the glomerulus transcriptomic profiling, patients with profound kidney dysfunction and those with an estimated glomerular filtration rate (eGFR) < 30 mL/min/1.73 m^2 were not considered for this study. As the controls, normal cortical tissues were again collected from the non-cancer-affected cortex of 22 renal carcinoma patients who exhibited

no evidence of chronic kidney disease.

2.3. Microdissection, RNA isolation, and RNA sequencing

Collected kidney tissues were manually microdissected under an EZ4 stereomicroscope (Leica, Wetzlar, Germany). An average number of 8 to 12 glomeruli were collected from each biopsy specimen for glomerulus RNA-seq. For tubulointerstitial RNA-seq, the author thoroughly removed glomerulus before collection of the microdissected tissue. Total RNAs were extracted from the microdissected glomeruli using an RNeasy micro kit (Qiagen, Hamburg, Germany). A SMARTer Ultra Low Input RNA Kit version 3 (Takara Bio, Mountain View, CA, USA) was used to construct complementary DNA libraries in glomerulus sequencing considering the low total amount of mRNA in the microdissected tissues. For tubulointerstitial RNA-seq, a TruSeq Stranded Total RNA Library Prep Kit (Illumina, CA, USA) was used to construct cDNA libraries. Paired-end RNA sequencing was performed on a Hiseq2500 platform (Illumina, San Diego, CA, USA) to obtain 100-base-

pair sequences.

2.4. RNA-seq profiling

FastQC was used for initial quality control. For glomerulus RNA-seq data, the author identified that low-quality nucleotides and adapter sequences take certain portion of the results, thus, the sequences were trimmed off using the cutadapt software.[5] The FASTQ reads were aligned to the human reference genome using the mapping program Bowtie 2 (version 2.1.0.0) or STAR (version 2.3.0).[6] To quantify gene expression, uniquely mapped reads were counted with featureCounts or HTseq software.[7,8]

2.5. Differentially expressed genes and pathway enrichment analysis

Genes with fewer than 20 reads in more than half of the samples were excluded from the downstream analysis. R packages factoextra and FactoMineR were used for principal components analysis.[9] Differentially expressed genes (DEGs) were called at Benjamini-Hochberg-adjusted false discovery

rate of 0.01 using the DESeq2 package (version 1.24.0).[10] Gene set enrichment analysis was performed with R packages pathview,[11] goseq,[12] and ToppGene Suite.[13] The annotated domains with a false discovery rate < 0.05 are presented. Heatmaps and correlation plots were drawn with the counts per million reads values of the genes of interest.

2.6. Glomerulus RNA-seq target gene selection for IgAN and experimental validation study

Of the identified DEGs, a target gene (spleen tyrosine kinase, SYK) was selected by literature review, and additional validation study with immunohistochemistry staining was performed in independent human IgAN kidney biopsy samples. The author first stained 22 independent IgAN samples from patients who met the same criteria as our sequenced IgAN samples. Then, 12 additional samples from IgAN patients with kidney dysfunction (eGFR < 60 mL/min/1.73 m^2) were stained with the same method to further evaluate the expression in IgAN patients with significantly decreased kidney function. Experimental 12 control samples consisted of biopsied kidney

tissues from insignificant finding in their biopsy reports, and without any laboratory evidence of kidney dysfunction. For staining, 4-μm paraffin-embedded tissue sections were deparaffinized with xylene and rehydrated with ethanol. Background signals were blocked with a Protein Block Serum-Free Ready-to-use blocking reagent (cat. no. X0909, Agilent, Santa Clara, CA, USA). Total and phosphorylated SYK proteins were probed with the respective primary antibodies (for total SYK, sc-1240 at 1:300 dilution, Santa Cruz Biotechnology, Dallas, TX, USA; for phosphor-SYK, #27115 at 1:200 dilution, Cell Signaling Technology, Danvers, MA, USA) at 4°C overnight. Images were captured using a Nikon Eclipse Ci inverted microscope (Nikon Imaging, Tokyo, Japan). Quantification of the immunohistochemical signals was performed with ImageJ (version 1.8.0, National Institutes of Health, Bethesda, MD, USA) to measure the proportion of stained area among the identified glomeruli. The measurement was performed in at least three glomeruli per sample, and the mean values were calculated.

For immunofluorescence staining, deparaffinized tissue slides

were labeled with primary antibodies against total SYK (sc-1240, at 1:300 dilution, Santa Cruz) and α-smooth muscle actin (αSMA; ab32575, at 1:300 dilution, Abcam, Cambridge, UK), followed by secondary antibodies (AlexaFluor goat anti-mouse 488 A1101 and goat anti-rabbit 555 A214228; Thermo Fisher Scientific, Waltham, MA, USA). 4',6-diamidino-2-phenylindole (DAPI) was used for nuclear counterstain. Confocal microscopy was performed on a TCS SP8 STED CW confocal microscope (Leica).

The author also used primary cultured human mesangial cells for *in vitro* experiments. Non-cancerous normal kidney tissues were obtained from patients who underwent nephrectomy for renal cell carcinoma, and the kidney cortices were mechanically dissected. The glomeruli were isolated using a series of 125-, 106- and 75- μm Fisherbrand U.S. Standard Test Sieves (Fisher Scientific, Thermo Fischer Scientific, Waltham, MA, USA) and cultured for 8 days. Outgrowing cells were detached by trypsin and passed through sieves to obtain glomerular cores enriched in mesangial cells. On day 8, 1×10^6 cells were incubated with an Fc receptor blocking reagent (1 μ

g/mL, BD Bioscience, San Jose, CA, USA),[14] followed by labeling with anti-CD90 monoclonal antibodies (cat. 12-0909-42, Thermo Fischer Scientific) and sorting on a BD FACSCalibur instrument (BD Biosciences). These cells were cultured in humid 5% CO_2 atmosphere at 37°C.

In the *in vitro* experiments, the author collected serum specimens from a healthy individual without any evidence of kidney disease and from an active IgAN patient with significant proteinuria (> 1g/g) but not receiving any immunosuppressive treatment. IgA1 molecules from the active IgAN patient isolated from serum using jacalin as reported before.[15] Cells were treated with either sera or patient-derived IgA1 for 48 hours after overnight starvation in multiple doses (6.25 to 200 μ g/mL). For immunoblotting, 80 μg of proteins were separated by electrophoresis on 10% sodium dodecyl sulfate-polyacrylamide gels and transferred onto Immobilon-FL 0.4-μ M polyvinylidene difluoride membranes (Millipore, Bedford, MA, USA). Proteins were probed with primary antibodies targeting phospho-SYK (Santa Cruz) and total-SYK (Cell Signaling Technology), followed by anti-rabbit IgG (Cell Signaling

Technology) secondary antibodies. The labeled proteins were detected by an enhanced chemiluminescence system (ECLTM PRN 2106; Amersham Pharmacia Biotech, Buckinghamshire, UK). Band intensities were analyzed using a Bio-Rad Gel Doc 1000 and Multi-Analyst version 1.1 (Bio-Rad Laboratories, Hercules, CA, USA). Quantification for western blot bands was performed with ImageJ, and the experiment was performed in quadruplets

For quantitative real-time PCR, total SYK mRNA was quantified in the primary cultured mesangial cells without treatment, with treatment of 500 μg/mL of isolated IgA1 from the jacalin method from a healthy individual, and with treatment of 500 μg/mL of isolated IgA1 from active IgAN patients as above. Total RNA was extracted from the mesangial cells by using the RNeasy kit, and 500 ng of total RNA was reverse-transcribed with oligo-d(T) primers and AMV-RT Taq polymerase (Promega, WI, USA). Real-time pCR was performed using either Assay-on-Demand TachMan probes or the SYBR Green method and primer for SYK (Applied Biosystems, Foster City, CA, USA) was used. The author used Applied Biosystems

PRISM 7500 sequence detection system for real-time PCR analysis. Relative quantification of the mRNA levels were performed by $2^{-\Delta\Delta CT}$, and the GAPDH served as a loading control. All *in vitro* experiments were performed in quadruplets.

The cells in above conditions as the real-time PCR was additionally experimented for their expression in Ki-67 to evaluate the proliferative activity of mesangial cells by immunofluorescence microscopy. Cells on cover glasses were washed with phosphate-buffered saline and fixed in 4% paraformaldehyde for 20 min. The fixed cells were permeabilized with 0.3% Triton X and stained with antibodies against Ki-67 (ABCAM) in blocking agent overnight at 4 °C. Otherwise, the immunofluorescence microscopy was performed as the method used for human samples, and performed in quadruplets.

To further test the mesangial cell proliferation activity, MTS assay (Promega) was performed to detect viable cells, and the relative proportion to untreated control cells was calculated. The MTS assay was performed in untreated control cells, mesangial cells treated from isolated IgA1 from healthy

individuals or from active IgAN patients (250 or 500 μg/mL). The experiment was performed in quintuplets.

2.7. Tubulointerstitial RNA-seq target gene selection and experimental validation study

For the validation experiment for the results in tubulointerstitial RNA-seq of various glomerulonephritis, the gene that showed the greatest difference based on the false discovery rate (i.e., dual-specificity phosphatase 1, *DUSP1*) was selected as the gene of interest for experimental validation. To ensure that gene expression was universally altered in the profiled kidney diseases, the author tested whether the expression level in each disease category was significantly different compared to that in the nephrectomy controls.

Immunohistochemical staining was performed on independent human kidney tissues. The author included samples from patients with major primary glomerulonephritis, specifically 32 patients with IgAN, 14 with membranous nephropathy, and 15 with minimal change disease. In addition, pathology slides from 24 nephrectomy controls were included. No patient had a

significantly reduced eGFR (< 60 mL/min/1.73 m^2). The author sliced paraffin-embedded, unstained tissue sections stored at the time of kidney biopsy or nephrectomy into 4-μm sections. After deparaffinization and rehydration with three incubations in xylene followed by a series of descending concentrations of ethanol, immunohistochemical staining was performed. To block nonspecific background staining, blocking reagent (Santa Clara, CA, USA) was used. In addition to *DUSP1*, kinases affected by *DUSP1* activity, including p38 and *ERK* were also targeted in this experiment. Staining with an antibody against *DUSP1,* phospho-p38*,* and phospho-*ERK* (Novus Biologicals, CO, USA) was conducted at 4°C overnight. Images were acquired using a light microscopy system (Leica Microsystems, Germany). The author quantified the staining results with ImageJ (version 1.8.0., National Institute of Health, USA).

For immunofluorescence staining, deparaffinized tissue slides were stained with a primary antibody against *DUSP1* (Novus Biologicals, CO, USA) followed by secondary antibodies (Alexa Fluor goat anti-mouse 488 (A1101) and goat anti-rabbit 555 (A214228); Thermo Fisher Scientific, Waltham, MA, USA). For

nuclear staining, 4',6-diamidino-2-phenylindole (DAPI) was used. Confocal microscopy was performed on a TCS SP8 STED CW confocal microscope (Leica Microsystems).

The author additionally performed an *in vitro* study, and primary cultured human tubular epithelial cells (hTECs) from the unaffected cortex of a nephrectomy control individual were obtained.[16] After mechanically dissecting the kidney cortices, the author isolated tubules with the sieving technique and cultured them for 8 days. The author trypsinized the outgrowing cells and collected cultured hTECs via additional sieving. On day 8, the cultured hTECs were counted, and 1×10^6 cells were incubated with Fc receptor blocking reagent (1 μg/mL, BD Bioscience, CA, USA). The author identified hTECs by labeling with anti-CD90 monoclonal antibodies (cat. 12-0909-42, Thermo Fischer Scientific) and sorting in a BD FACSCalibur instrument (BD Bioscience). The sorted cells were cultured in a humidified 5% CO_2 atmosphere at 37°C.

With the hTECs, the author performed western blot analysis and evaluated the *DUSP1*-related molecular pathways with altered *DUSP1* activity. As *DUSP1* suppresses the activity of

p38, its target molecules include not only p38 but also the molecules in the downstream c-Jun (JUN)/c-Fos (FOS) pathway (including JUN, FOS, and c-Jun N-terminal kinase (JNK)) and extracellular signal-regulated kinase (ERK).[17] In addition, the downstream transcription factor activated protein 1 (AP-1) was evaluated. The author treated hTECs with TNFα to mimic tubulointerstitial inflammation, because evidence indicates that this molecule plays a role in various kidney diseases.[18-20] hTECS were stimulated with TNFα at a concentration of 10 ng/mL for 1 hour.

For western blot analysis, the author extracted total protein and separated equal amounts (80 μg) of protein on 10% sodium dodecyl sulfate (SDS)-polyacrylamide gels and transferred them onto Immobilon-FL 0.4 μM polyvinylidene difluoride membranes (Millipore, MA, USA). Primary antibodies against β-actin (Sigma-Aldrich, MO, USA), DUSP1 (Novus Biologicals), p38 (Cell Signaling Technology, MA, USA), phospho-p38 (Cell Signaling Technology), JNK (Cell Signaling Technology), phospho-JNK (Cell Signaling Technology), ERK (Cell Signaling Technology), phospho-ERK (Cell Signaling Technology), JUN

(Cell Signaling Technology), phospho-JUN (Cell Signaling Technology), FOS (Cell Signaling Technology), phospho-FOS (Cell Signaling Technology), AP-1 (MyBioSource, CA, USA), and phospho-AP1 (MyBioSource) were used. The author used an anti-rabbit IgG secondary antibody (Cell Signaling Technology). Quantification of western blot band densities was performed with ImageJ, and the relative levels of DUSP1 and phosphoproteins were calculated by dividing these levels by the expression level of β-actin and the expression levels of the corresponding total forms.

BCI is an allosteric inhibitor of DUSP1/6, and its effect on various disease conditions has been shown.[21,22] The author first confirmed the appropriate BCI concentration for the experiment by adding BCI (Millipore) at 1.25 mM, 2.5 mM, and 5.0 mM to the culture medium of hTECs for 3 hours and then stimulating the hTECs with TNFα. The BCI concentration considered to sufficiently increase p38 expression was used for the main experiment. Next, the author tested the effects of pharmacologic inhibition by BCI in cells with no treatment, with BCI treatment only, with TNFα stimulation only, and with TNFα

stimulation after treatment with BCI at the determined concentration for 3 hours.

The author used custom-manufactured adenovirus for *in vitro* transduction of *DUSP1* (adeno-*DUSP1*, Sirion Biotech, Germany) to overexpress *DUSP1* in hTECs. The author first confirmed the appropriate multiplicity of infection (MOI) for *DUSP1* overexpression by transducing cells with adeno-DUSP1 at MOIs of 10, 25, and 50 for 24 hours and assessing phospho-p38 and DUSP1 levels. Next, the author assessed the relative levels of the target molecules in cells transduced with control adenovirus, transduced with adeno-*DUSP1*, stimulated with TNFα, and stimulated with TNFα after adenovirus-mediated overexpression of *DUSP1*.

As previous studies suggested that glucocorticoids act through *DUSP1* to exert their effects on p38 and related pathways, the author further sought to determine whether specifically targeting *DUSP1* may be helpful for reducing the glucocorticoid dosage while maintaining immunosuppressive efficacy in hTECs. First, to confirm the dexamethasone concentration, the author assessed phospho-p38 and DUSP1

levels in tics treated with 0.25, 0.5, and 1.0 mM dexamethasone (Sigma-Aldrich) for 1 hour and then stimulated with TNFα. Next, the author treated TNFα-stimulated hTECs with a low concentration and a high concentration of dexamethasone and assessed the relative levels of the target molecules. In addition, hTECs transduced with adeno-DUSP1 at an MOI of 50 for 24 hours were treated with the low concentration of dexamethasone and then stimulated with TNFα.

Chapter 3. Results - glomerulus RNA-seq

3.1. Clinical characteristics and exploratory analysis

Outliers in one each of the study and the control group were excluded according to principal component analysis results. The clinical features of the finally included 14 IgAN patients and 10 controls are shown in Table 1. The median eGFR was 81.6 mL/min/1.73 m^2, and the median random urine protein-creatinine ratio was 1.1 g/g.

Table 1. Clinical characteristics of the study population for glomerulus RNA-seq.

ID	Age	Sex	Cr (mg /dL)	eGFR (mL/min /1.73 m^2)	UPCR (g/g)	M	E	S	T	C
IgAN1	58	M	1.0	74.9	0.5	0	0	0	0	0
IgAN2	26	M	0.9	93.4	0.5	0	0	1	0	0
IgAN3	33	F	0.8	82.2	0.9	1	1	1	0	1
IgAN4	18	M	0.7	138.6	0.2	0	1	1	0	0
IgAN5	34	F	0.8	80.9	0.4	0	0	1	0	0
IgAN6	32	M	1.0	78.0	0.7	0	1	1	0	0
IgAN7	41	M	1.1	68.5	2.9	1	1	1	0	0
IgAN8	32	M	1.2	69.6	2.8	1	0	1	2	0
IgAN9	35	M	1.1	76.0	1.7	1	1	1	0	0
IgAN10	47	M	0.9	83.4	1.2	1	0	1	0	0
IgAN11	57	M	1.0	73.7	1.6	1	1	0	0	0
IgAN12	37	F	0.4	145.0	1.9	0	0	0	0	0
IgAN13	20	M	0.9	101.2	1.0	1	1	0	0	0
IgAN14	36	F	0.5	117.2	2.0	-	-	-	-	0
Control1	43	M	0.9	83.7	-	-	-	-	-	-
Control2	57	F	0.6	100.8	-	-	-	-	-	-
Control3	60	M	0.9	83.7	-	-	-	-	-	-
Control4	31	F	0.6	106.3	-	-	-	-	-	-
Control5	62	M	0.8	92.4	-	-	-	-	-	-
Control6	49	F	0.6	98.6	-	-	-	-	-	-
Control7	37	M	0.9	91.1	-	-	-	-	-	-
Control8	43	M	0.9	87.3	-	-	-	-	-	-
Control9	58	M	0.9	78.7	-	-	-	-	-	-
Control1	55	M	0.7	105.1	-	-	-	-	-	-

Each sample yielded 25,330,450 ~ 48,226,631 paired-end RNA-seq reads, of which 18,244,340 ~ 42,925,026 reads (72.0 ~ 91.0 percent) were mapped to Ensembl-annotated exons. After filtering out lowly expressed genes, the author found that 16,438 Ensembl genes were expressed in our samples. To ensure that our FASTQ sequences were enriched in glomerulus-specific genes, the author examined expression levels for select gene markers for the glomerulus, proximal tubule, and collecting duct. Figure 1 illustrates representative RNA-seq histograms for a few selected examples of glomeruli- or tubule-specific transcripts, as displayed on the UCSC Genome Browser [23]. The average expression levels for nephrin (*NPHS1*), podocin (*NPHS2*), and podocalyxin (*PODXL*) were high [801.1, 6336.1, and 6430.2, and in average counts per million, respectively], whereas those for tubule- or collecting duct-specific transcripts such as aquaporin-1 (*AQP1*), uromodulin (*UMOD*), and aquaporin-2 (*AQP2*) were relatively low or absent (502.3, 333.3, and 54.6 in average counts per million, respectively). These results indicate that our manual microdissection and subsequent RNA-seq library construction

successfully captured human glomeruli from the human biopsy samples with removal of abundant tubule tissues.

Figure 1. Expression of structure-specific genes.

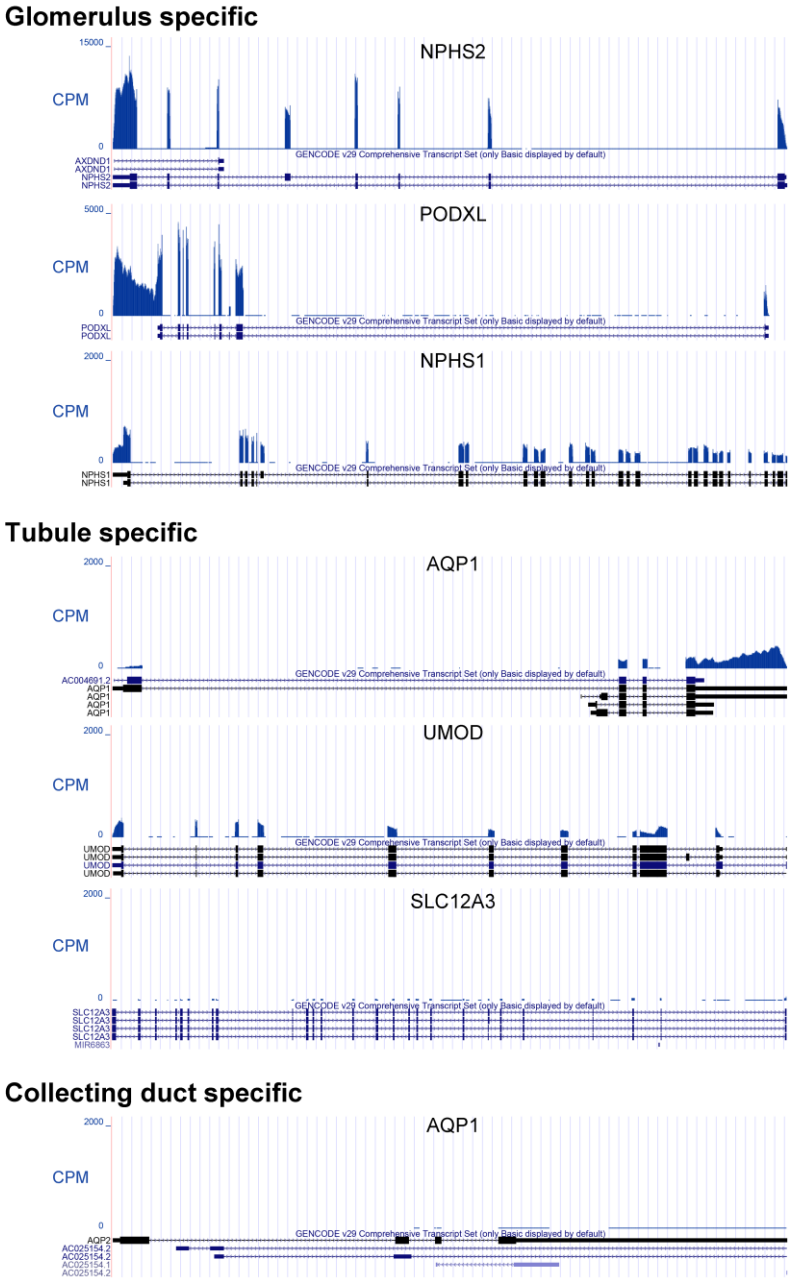

Representative snapshots from the UCSC genome browser show that RNA-seq libraries generated from microdissected glomeruli were highly enriched for glomerulus-specific reads. Dark-blue histograms represent RNA-seq reads mapped to the exons. The y-axes for NPHS1, AQP1, UMOD, SLC12A3, and AQP2 were on the same scale.

Next, global patterns of gene expression were analyzed in an unsupervised manner to detect covariates that may explain variability in our samples. Principal component analysis shows a clear separation between control and IgAN groups, with the first and second principal components explaining 20.5% and 11.1% of variability, respectively (Figure 2A). A gene-wise principal-component plot demonstrates genes with the highest variability between two groups (Figure 2B).

Figure 2. Principal component analysis results.

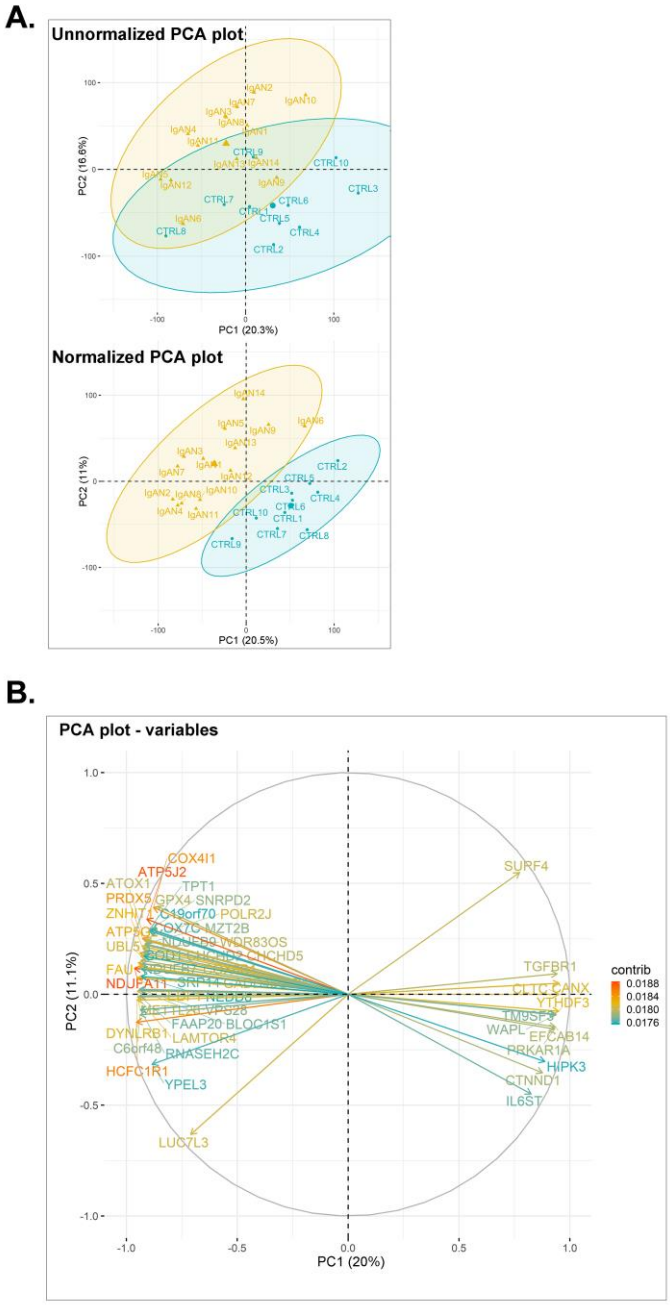

A. Principal component analysis showed that the IgAN patients and the controls are relatively well-separated regarding the major principal components. B. Principal component analysis showing the gene expressions that had high contribution regarding the calculated eigen values. PC, principal component; PCA, principal component analysis.

3.2. Genes differentially expressed in the glomeruli of IgAN patients

To identify genes differentially expressed in the IgAN samples, the author modeled RNA-seq count data using a negative binomial distribution and determined adjusted *P*-values [i.e., false discovery rate (FDR)] using a Wald test [10]. The author identified 2,497 DEGs, of which 1,380 genes were upregulated and 1,117 genes downregulated in the IgAN group (FDR < 0.01), shown in Figure 3A, and Figure 3B is a heatmap drawn from representative DEGs associated with several canonical molecular pathways.

Figure 3. Differentially expressed genes in the IgAN patients.

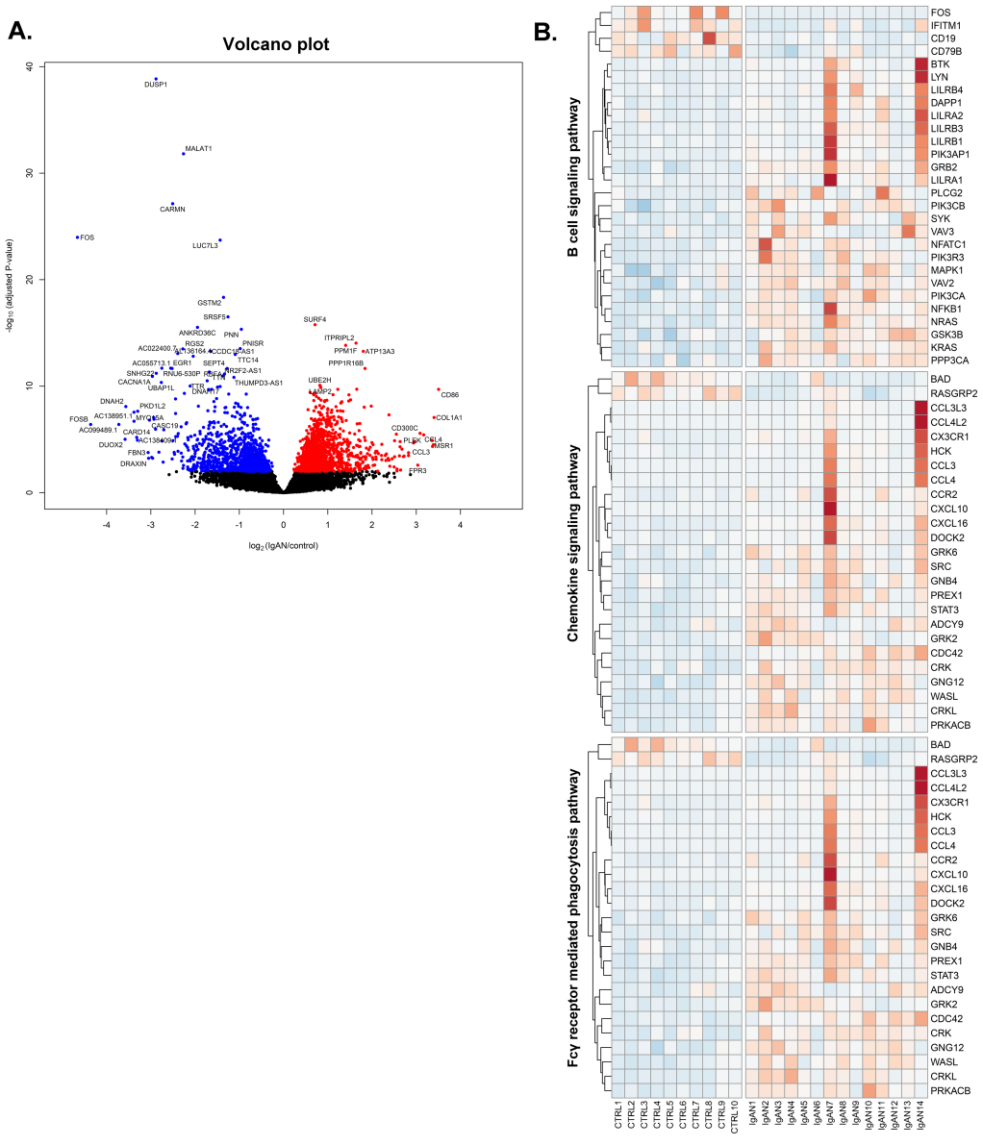

A. A volcano plot showing genes differentially expressed in IgAN samples. Adjusted P-value < 0.01 was used as a threshold for statistical significance and the significant differentially expressed genes were colored; red dots indicate the upregulated genes and blue dots indicate the downregulated genes. Gene names were shown for the significantly differentially expressed genes with adjusted P-value < 10^{-10} or log2 fold-change absolute value > 3. B. A heatmap showing the relative expression levels of differentially expressed genes in the notable pathways among the study subjects. The gene expression levels were normalized by the DESeq2 method. The expression levels are scaled and clustered by the Euclidian method by rows (genes).

Table 2 lists representative genes whose expression was significantly altered in the glomeruli of the IgAN group.

Table 2. Representative DEGs in IgAN glomerulus.

Genes	Protein names	Median expression	Log2 fold changes (IgA/Control)	False discovery rate
Upregulated genes				
CCL3	C-C motif chemokine ligand 3	339.87	3.37±0.7	4.52E-05
CCL4	C-C motif chemokine ligand 4	1014.07	3.39±0.69	3.11E-05
CXCL16	C-X-C motif chemokine ligand 16	1558.01	1.3±0.21	8.96E-08
BTK	Bruton tyrosine kinase	134.54	2.38±0.6	8.81E-04
SYK	spleen associated tyrosine kinase	524.80	1.13±0.23	2.33E-05
MAPK1	Mitogen-activated protein kinase 1	2815.94	0.43±0.12	0.002
TNF	Tumor necrosis factor	39.56	1.83±0.54	0.006
TGFBR1	transforming growth factor beta receptor 1	1092.81	1.3±0.19	3.64E-09
SMAD3	SMAD family member 3	845.58	0.75±0.15	1.08E-05
SMAD5	SMAD family member 5	1467.68	0.56±0.16	0.004
COL1A1	collagen type I alpha 1 chain	1208.42	3.4±0.55	8.42E-08
C4A	complement C4A	210.56	1.98±0.3	7.01E-09
C4B	complement C4B	208.68	2.38±0.38	4.75E-08
B4GALT1	beta-1,4-galactosyltransferase 1	772.57	1.10±0.23	5.68E-05
PIK3CA	phosphatidylinositol-4,5-bisphosphate 3-kinase catalytic subunit alpha	711.62	0.83±0.18	8.30E-05
AKT1	AKT serine/threonine kinase 1	1748.44	0.75±0.29	0.039
HIF1A	hypoxia inducible factor 1 alpha subunit	3025.80	0.51±0.17	0.015
GRK2	G protein-coupled receptor kinase 2	1309.16	1.15±0.24	3.64E-05
Downregulated genes				

DUSP1	dual specificity phosphatase 1	14442.76	-2.88±0.21	1.66E-39
MALAT1	metastasis associated lung adenocarcinoma transcript 1	144833.63	-2.26±0.18	1.73E-32
CARMN	cardiac mesoderm enhancer-associated non-coding RNA	440.55	-2.51±0.21	7.56E-28
FOS	Fos proto-oncogene, AP-1 transcription factor subunit	3447.93	-4.66±0.42	1.09E-24
FOSB	FosB proto-oncogene, AP-1 transcription factor subunit	223.33	-4.36±0.74	3.86E-07
JUNB	JunB proto-oncogene, AP-1 transcription factor subunit	3373.22	-1.81±0.32	7.48E-07
AGTR1	angiotensin II receptor type 1	1604.62	-1.56±0.26	2.93E-07
RGS2	regulator of G protein signaling 2	1564.64	-2.28±0.27	3.17E-14
RGS11	regulator of G protein signaling 11	220.85	-1.12±0.28	0.001
RGS16	regulator of G protein signaling 16	321.37	-1.58±0.28	7.37E-07

Among the upregulated genes were genes known to associate with inflammation and immune cell mobilization. For example, pro-inflammatory chemokines such as *CCL3*, *CCL4*, and C-X-C motif chemokine ligand 16 *(CXCL16)* were upregulated in IgAN glomeruli. Genes involved in the B cell and Fcɣ receptor pathways such as Bruton tyrosine kinase (*BTK)*, spleen tyrosine kinase (*SYK*), and mitogen-activated protein kinase 1 (*MAPK1*) were upregulated in the IgAN group. Transcripts for molecular mediators involved in the pro-fibrotic TGFβ signaling pathway were also upregulated in the IgAN group, including tumor necrosis factor (*TNF)*, transforming growth factor beta receptor 1 (*TGFBR1)*, SMAD family member 3 (*SMAD3)*, *SMAD5* or collagen type I alpha 1 chain (*COL1A1*). Genes related to PI3K-AKT pathway, also a known pathway related to inflammation, such as G protein-coupled receptor kinase 2 (*GRK2*),[24] hypoxia inducible factor 1 alpha subunit (*HIF1A*),[25] phosphatidylinositol-4,5-bisphosphate 3-kinase catalytic subunit alpha (*PI3KCA*), were enriched in IgAN glomeruli. Also, certain complement genes, including *C4A* and *C4B*, and β1,4-galactosyltransferase (*B4GALT1*), a recently

proposed receptor for IgA in human mesangial cells,[26] were significantly upregulated in the IgAN transcriptome. These findings provide evidence that glomerular inflammation and the initiation of fibrosis take place in the glomerulus of IgAN patients with relatively preserved kidney function.

When the author investigated the downregulated genes, dual specificity phosphatase 1 (*DUSP1*), a negative regulator of MAPK pathway, and metastasis-associated lung adenocarcinoma transcript 1 (*MALAT1*), cardiac mesoderm enhancer-associated non-coding RNA (*CARMN*), and Fos proto-oncogene (*FOS*) were the genes with the lowest FDR. FosB proto-oncogene (*FOSB*), JunB proto-oncogene (*JUN*), related to the FOS-JUN pathway, were also downregulated in the IgAN glomeruli transcriptome. Angiotensin receptor type 1 (*AGTR1*), as previously reported with mesangial cells,[27] was downregulated in IgAN glomeruli. In addition, regulator of G protein signaling 2 (*RGS2*), *RGS16*, *RGS 11*, were downregulated, implying that regulations for inflammatory signals might have been reduced, further suggesting a pro-inflammatory state in IgAN glomerulus.

3.3. Gene ontology enrichment and pathway analysis

To further define biological processes and functions of the differentially expressed transcripts, the author performed Gene Ontology (GO) terms annotation and mapped up- and down-regulated genes onto a set of molecular pathways annotated in the Kyoto Encyclopedia of Genes and Genomes (KEGG) database. Table 3 summarizes the top 10 highly overrepresented GO terms in each biological process, cellular component, and molecular function GO category in the IgAN transcriptome as compared with controls. The enriched GO terms in the biological process category included cellular motility/migration, protein/vesicle transport, and immune system. Overrepresented GO cellular components terms included junction, Golgi apparatus, vacuole, and endoplasmic reticulum. Enzyme or kinase binding, nucleoside, ribonucleoside or nucleotide binding were the molecular function GO terms that were overrepresented in IgAN transcriptome. KEGG pathway analysis for differentially expressed genes revealed that canonical molecular pathways involved in B cell signaling, chemokine signal transduction, and

FcγR-mediated phagocytosis were overrepresented (Figure 4).

Table 3. Gene ontology (GO) term annotation results.

GO ID	Name	Genes in Annotation	Genes from Input	FDR (Bonferroni)
Biological Process				
GO:0016192	vesicle-mediated transport	1,514	215	< 0.001
GO:0040011	locomotion	1,735	215	< 0.001
GO:0016477	cell migration	1,300	173	< 0.001
GO:0015031	protein transport	1,948	230	< 0.001
GO:0048870	cell motility	1,428	181	< 0.001
GO:0051674	localization of cell	1,428	181	< 0.001
GO:0006955	immune response	1,572	194	< 0.001
GO:0007169	transmembrane receptor protein tyrosine kinase signaling pathway	700	108	< 0.001
GO:0002682	regulation of immune system process	1,506	187	< 0.001
GO:0002684	positive regulation of immune system process	97	136	< 0.001
Cellular component				
GO:0005912	adherens junction	484	93	< 0.001
GO:0070161	anchoring junction	503	95	< 0.001
GO:0005773	Vacuole	1,223	171	< 0.001
GO:0005794	Golgi apparatus	1,518	197	< 0.001
GO:0005925	focal adhesion	393	75	< 0.001
GO:0005924	cell-substrate adherens junction	398	75	< 0.001
GO:0005783	endoplasmic reticulum	1,706	205	< 0.001
GO:0044437	vacuolar part	700	108	< 0.001
GO:0030055	cell-substrate junction	403	75	< 0.001
GO:0000139	Golgi membrane	716	109	< 0.001
Molecular function				
GO:0019899	enzyme binding	1,929	253	< 0.001
GO:0019900	kinase binding	691	104	< 0.001
GO:0019901	protein kinase binding	620	96	< 0.001
GO:0035639	purine ribonucleoside triphosphate binding	1,815	202	< 0.001
GO:0032550	purine ribonucleoside binding	1,828	203	< 0.001

GO:0001883	purine nucleoside binding	1,831	203	< 0.001
GO:0032549	ribonucleoside binding	1,831	203	< 0.001
GO:0001882	nucleoside binding	1,838	203	< 0.001
GO:0032555	purine ribonucleotide binding	1,864	205	< 0.001
GO:0017076	purine nucleotide binding	187	206	< 0.001

Figure 4. Three notable differentially expressed KEGG pathways in the IgAN patients.

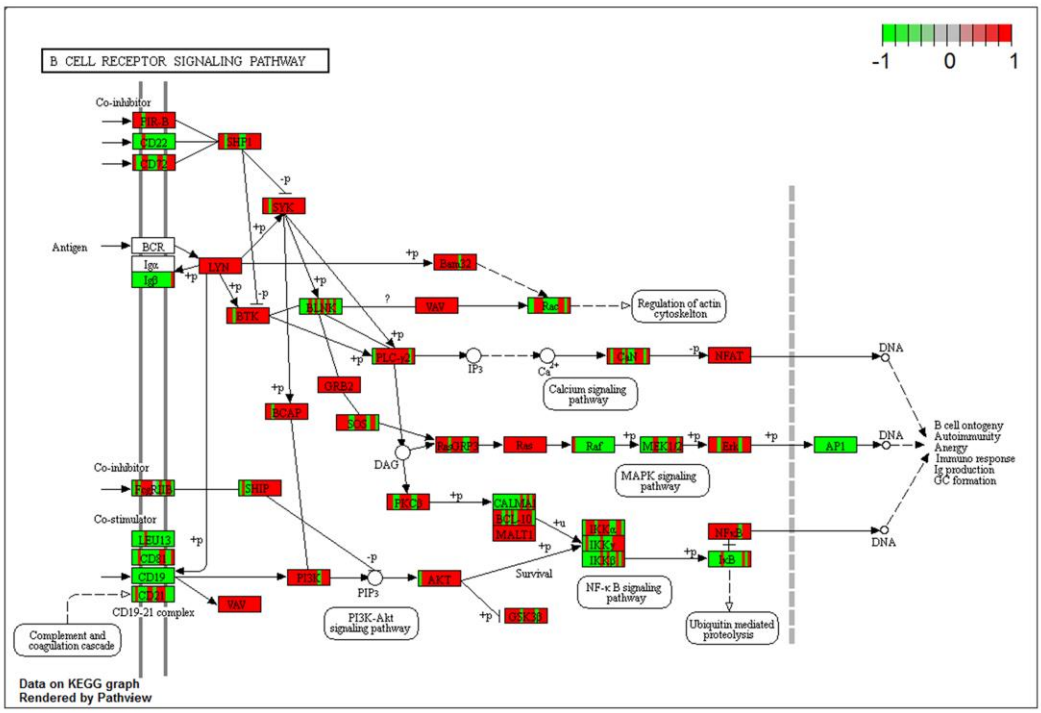

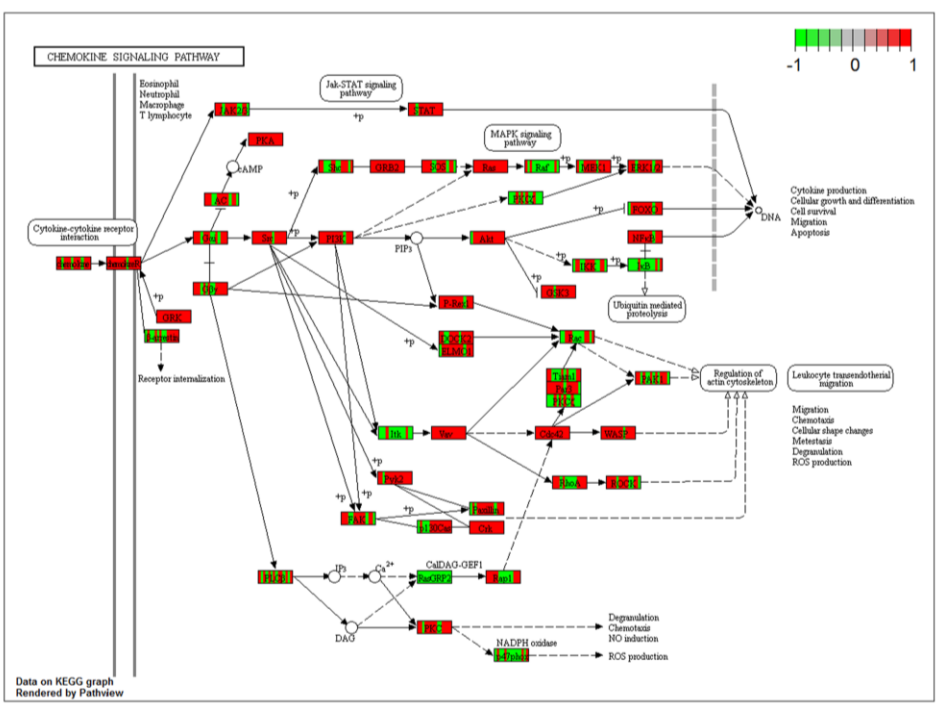

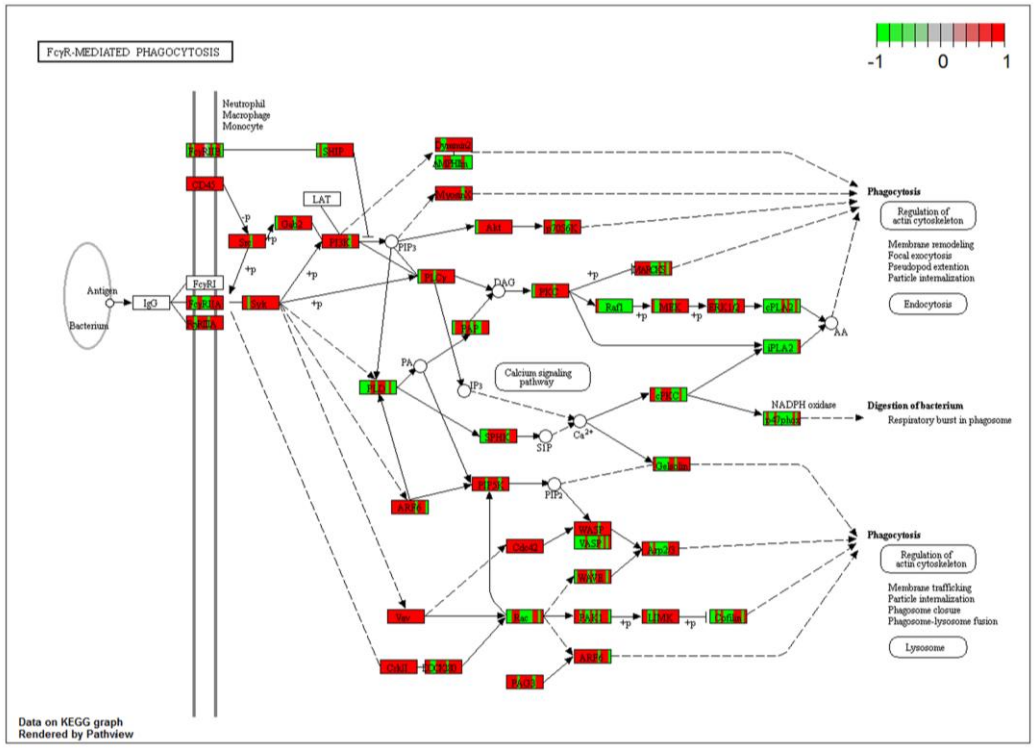
FcγR-MEDIATED PHAGOCYTOSIS
-1
0
1
Neutrophil
Macrophage
Monocyte
LAT
Antigen
Bacterium
IgG
FcγRI
Syk
PIP3
DAG
PKC
Raf1
MEK
ERK1/2
cPLA2
AA
PLA2
PLCγ
PA
IP3
Calcium signaling pathway
NADPH oxidase
Digestion of bacterium
Respiratory burst in phagosome
SIP
Ca2+
PIP2
ARF6
Cdc42
Rac
Phagocytosis
Regulation of actin cytoskeleton
Membrane remodeling
Focal exocytosis
Pseudopod extention
Particle internalization
Endocytosis
Membrane trafficking
Particle internalization
Phagosome closure
Phagosome-lysosome fusion
Lysosome
Data on KEGG graph
Rendered by Pathview

3.4. *In vivo* spleen tyrosine kinase expression in IgAN glomeruli

Based on the prior reports[15,28,29] and our RNA-seq results, the author sought to explore the role of spleen tyrosine kinase (SYK). Within the transcriptome of IgAN patients, SET binding factor 1 (*SBF1*), oxysterol-binding protein-related protein 11 (*OSBPL11*), AC138409.2, tripartite motif-containing protein 14 (*TRIM14*), serine/threonine-protein kinase pim-1 (*PIM1*), Ras-related protein 21 (*RAB21*), tribbles pseudokinase 1 (TRIB1) showed Pearson R^2 values over 0.5 with the expression levels of SYK, thus, considered as genes whose expressions were correlated with that of SYK.

In addition, immunochemical labeling of glomerular SYK in kidney biopsies obtained from an independent set of IgAN patients revealed that expression of SYK was upregulated, but the differences between the control and the IgAN patients without profound kidney dysfunction were small (Figure 5A). On immunofluorescence, intra-glomerular expression of SYK was detected in the mesangial area or infiltrating leukocytes (Figure 5B). When the author expanded our study samples to

include advanced IgAN cases with overt kidney dysfunction, a significant difference between the IgAN and control samples were detected regarding total and phosphor-SYK (Figure 5C). Notably, the author observed that cellular crescents in IgAN glomeruli exhibited strong signals for both phospho- and total-SYK.

Figure 5. *In vivo* validation of the intraglomerular expression of spleen tyrosine kinase (SYK).

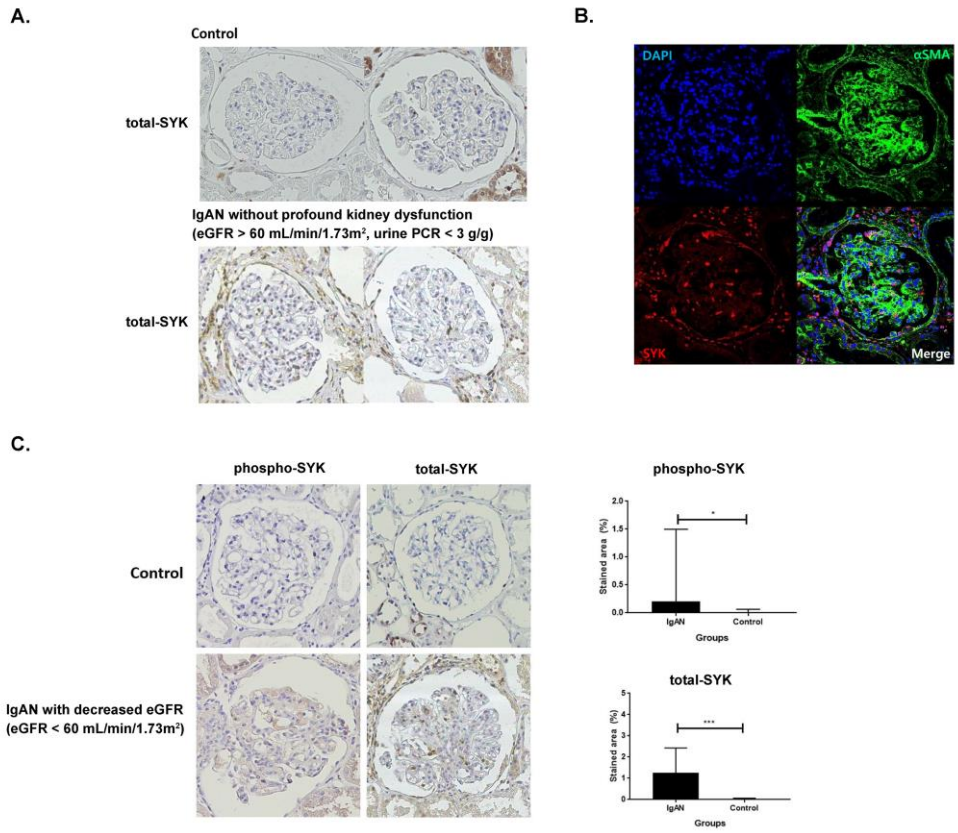

A: In the samples from IgAN patients without profound kidney dysfunction, the expression of total SYK did not show a significant difference from those in the controls. B: Confocal immunofluorescence microscopic images show that SYK colocalizes with mesangial cell marker alpha-smooth muscle actin (αSMA). C: IgAN samples obtained from patients with reduced eGFR (< 60 mL/min/1.73 m^2) exhibited a significantly higher expression of both total and phosphorylated SYK. Interestingly, a crescent with a strong SYK signal was observed in an IgAN sample. * $P < 0.05$, ** $P < 0.01$.

3.5. *In vitro* study results

In primary cultured hMCs, the expression of total SYK did not change significantly with the addition of unpurified serum from a healthy individual or IgAN patient (Figure 6A). However, the expression of phospho-SYK was increased when hMCs were treated with serum from the IgAN patient, and this was not observed with serum from the control. After the hMCs were treated with isolated IgA1, the expression of phospho-SYK was increased in a concentration-dependent manner (Figure 6B). Further, when the author performed quantitative real-time PCR assay in mRNA level, the mRNA level of total SYK was increased by patient-isolated IgA1 (Figure 6C) but not by isolated IgA1 from a healthy individual (Figure 6C). The treatment of patient-derived IgA1 also resulted in increase in mesangial cell proliferation identified by expression of Ki-67 (Figure 6D). The above *in vitro* results indicate that SYK is one of the molecules that are increased in mesangial cells by signals initiated by IgA1 in IgAN patients, along with the increased proliferation of mesangial cells.

Figure 6. *In vitro* experiment results in primary culture of human mesangial cells.

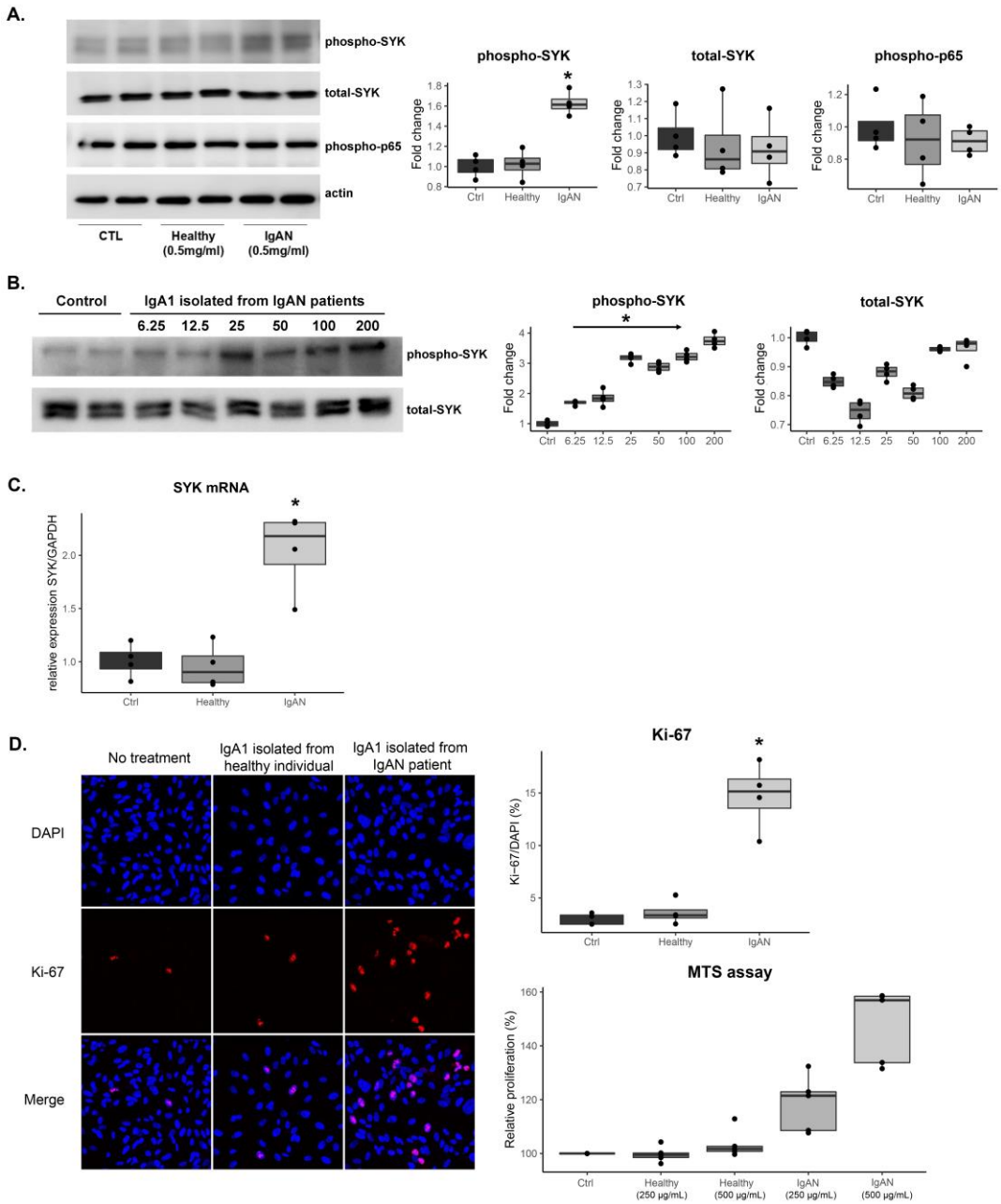

A: Primary human mesangial cells treated with IgA isolated from the IgAN patient's serum expressed higher amount of phosphorylated SYK (phosphor-SYK), without a significant change in the total amount of SYK. B: Patient-derived IgA1 increased the phosphorylated form of SYK in a dose-

dependent manner without causing an increase in the total amount of SYK. The statistical significance for the positive association was tested by the Pearson's correlation test. The experiment was conducted in quadruplets and the representative images were shown. C: Quantitative real-time PCR results for total SYK indicated that total SYK mRNA levels were increased by treatment of patient-derived IgA1 but not by IgA1 isolated from a healthy individual (dose: 500 μg/mL). The experiment was conducted in quadruplets. D: Expression of Ki-67 evaluated by confocal microscopy showed that mesangial cell proliferation activity was increased by patient-derived IgA1 but not by IgA1 from healthy individual (dose: 500 μg/mL). The experiment was conducted in quadruplets and the representative image is shown. In addition, MTS assay (quintuplets) was performed to evaluate the proliferation activity of the mesangial cells. Mesangial cells were untreated (Ctrl), treated from isolated IgA1 from healthy individual, or treated from isolated IgA1 from active IgAN patient (250 or 500 μg/mL). The relative expression to the untreated control was presented. *$P < 0.05$, ** $P < 0.01$, *** $P < 0.001$.

Chapter 4. Results – tubulointerstitial RNA-seq

4.1. Clinical characteristics of the study patients

The clinical characteristics of the profiled individuals are presented in Table 4. The profiled patients exhibited largely preserved kidney function (eGFR ≥ 60 mL/min/1.73 m^2); 5 study patients—one with IgAN, one with diabetic nephropathy, one with focal segmental glomerulosclerosis, and two with minimal change disease—had an eGFR < 60 mL/min/1.73 m^2. The lupus nephritis patients had the youngest age range and the highest median eGFR value, while the minimal change disease and membranous nephropathy patients had a relatively high median urine protein-to-creatinine ratio (above 10 g/g). A total of 3 kidney disease patients—2 minimal change disease patients and one focal segmental glomerulosclerosis patient—had been treated with immunosuppressants before kidney biopsy.

Table 4. Baseline characteristics of the study population for tubulointerstitial RNA-seq.

Groups	Control	IgA nephropathy	Minimal change disease	Membranous nephropathy
Number of individuals	22	43	9	4
Age (years)	55 [49;60]	42 [32;49]	61 [38;75]	63 [57;68]
Sex				
Female	8 (36.4%)	22 (51.2%)	5 (55.6%)	1 (25.0%)
Male	14 (63.6%)	21 (48.8%)	4 (44.4%)	3 (75.0%)
Body mass index (kg/m2)	24.4 [22.8; 25.5]	22.5 [20.5; 24.5]	25.7 [22.8; 26.5]	25.0 [24.6;25.4]
Creatinine (mg/dL)	0.8 [0.7; 0.9]	0.9 [0.8; 1.0]	0.8 [0.7; 1.0]	0.7 [0.5; 0.8]
eGFR (mL/min/1.73 m^2)	96.0 [86.0; 105.0]	88.2 [75.3; 105.8]	78.1 [61.9; 106.9]	97.5 [89.4;107.8]
Urine protein-to-creatinine ratio	-	0.9 [0.5; 1.7]	11.4 [9.7; 15.7]	14.2 [6.1;19.6]
Hypertension	9 (40.9%)	14 (32.6%)	2 (22.2%)	2 (50.0%)
Diabetes mellitus	1 (4.5%)	2 (4.7%)	0 (0.0%)	0 (0.0%)
Immunosuppressant use before biopsy	0 (0%)	0 (0%)	2 (22.2%)	0 (0%)

(continued...)

Groups	Focal segmental glomerulosclerosis	Diabetic nephropathy	Lupus nephritis
Number of individuals	3	3	3
Age (years)	68 [54;69]	61 [57;63]	30 [25;32]
Sex			
Female	1 (33.3%)	3 (100.0%)	2 (66.7%)
Male	2 (66.7%)	0 (0.0%)	1 (33.3%)
Body mass index (kg/m2)	22.8 [22.4; 24.5]	24.4 [22.8; 24.6]	23.3 [21.2; 24.4]
Creatinine (mg/dL)	0.7 [0.7; 1.2]	0.7 [0.7; 0.9]	0.7 [0.5; 0.7]
eGFR (mL/min/1.73 m^2)	81.5 [61.0; 100.7]	84.2 [70.9; 91.9]	126.2 [126.2;133.0]
Urine protein-to-creatinine ratio	2.7 [2.6; 6.0]	3.3 [2.6; 5.2]	5.1 [3.1; 6.2]
Hypertension	3 (100.0%)	1 (33.3%)	1 (33.3%)
Diabetes mellitus	1 (33.3%)	3 (100.0%)	0 (0.0%)
Immunosuppressant use before biopsy	1 (33.3%)	0 (0%)	1 (33.3%)

4.2. Explanatory analysis results.

In our RNA-seq profiling data, the samples showed a > 90% mapping rate to Ensembl-annotated exons with a median of 34,032,131 (interquartile range, 31,211,550-37,958,876) mapped reads. After filtering out the genes with low expression, 16,164 genes were included in the downstream analysis. The normalized counts per million reads values were relatively low for glomerulus-specific genes, including nephrin (*NPHS1)* and podocin (*NPHS2*), but were relatively high for tubule-specific genes, including aquaporin 1 (*AQP1*), uromodulin (*UMOD*), solute carrier family 12 member 3 (*SLC12A3*), and *AQP2* (Figure 7). Specifically, these results implied that the gene expression profile of the tubulointerstitium was successfully acquired via our microdissection technique with minimal contamination by glomeruli. The global patterns of gene expression were investigated by principal component analysis, and some overlap was noted between the kidney disease group and the nephrectomy control group based on the first and second principal components.

Figure 7. Principal component analysis results and expression of structure-specific genes.

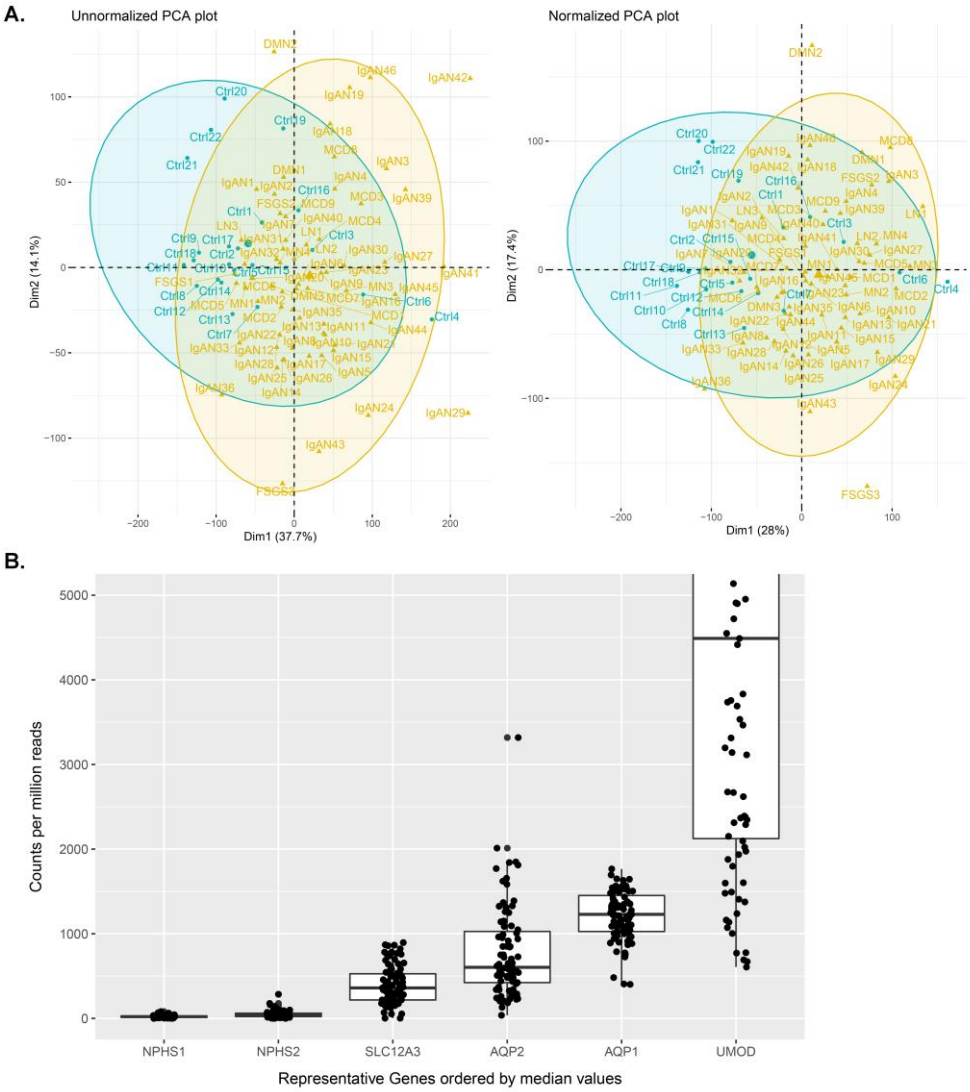

A: Principal components analysis with unnormalized and normalized read counts were performed and plots were drawn by the first and second principal components. B: The counts per million reads values of structure-specific genes expressions. The expressions of glomerulus-specific NPHS1 or NPHS2 were markedly low in the manually dissected tubule tissues, suggesting that the microdissection procedure successfully isolated tubules and glomerulus.

4.3. DEG analysis results.

The author identified 3037 genes with low expression and 2852 genes with high expression with a false discovery rate < 0.05 (Figure 1A). Among these genes, 142 genes with low expression showed a log2 fold change value < -1, and 383 genes with high expression showed a log2 fold change value ≥ 1. The significantly downregulated genes with the greatest absolute log2 fold change rates were *FOS*, nuclear receptor subfamily 4 group A member 1 (*NR4A1*), *NR4A2*, *NR4A3*, early growth response 1 (*EGR1*), and *DUSP1*, and *DUSP1* showed the lowest false discovery rate (7.03E-132). The significantly upregulated genes with the greatest log2 fold change were immunoglobulin heavy chain variable (*IGHV*) genes. The overall false discovery rates for the upregulated genes were larger than those for the downregulated genes, and ATP binding cassette subfamily G member 1 (*ABCG1*) had the lowest false discovery rate (4.10E-17).

Figure 8. Volcano plot for the DEG analysis results in tubulointerstitial RNA-seq.

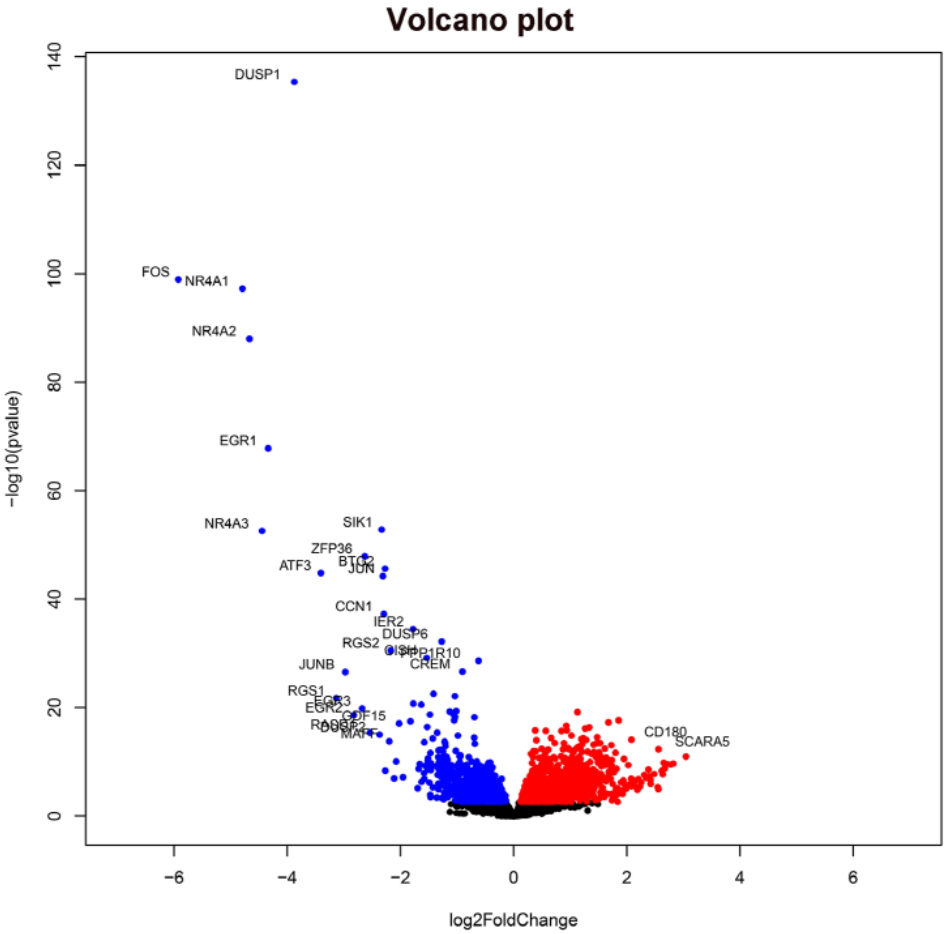

Volcano plot showing the differentially expressed genes. The differentially expressed genes with a false discovery rate < 0.05 are colored blue (for genes with low expression) and red (for genes with high expression)

4.4. Gene ontology enrichment analysis

There were 844 gene ontology domains (46 molecular function, 749 biological processes, 49 cellular components) annotated by the highly expressed DEGs and 250 domains (33 molecular function, 215 biological process, 2 cellular component) by the lowly expressed DEGs, respectively. Regarding the genes with low expression, notable significantly enriched gene ontology molecular function domains included MAP kinase or protein kinase pathways, transcription factor activity-related pathways, and pathways related to glucocorticoid receptor activity. Diverse biological process gene ontology terms were identified, and notable terms included cellular response to stimulus and negative regulation of MAP kinase or related pathways. Transcription factor AP-1 complex (GO:0035976) and nuclear chromatin (GO:0000790) were the cellular component gene ontology terms that were enriched with the significantly downregulated genes with log2 fold change < -1.

For the highly expressed genes, chemokine or cytokine activity-related pathways were notable molecular function

gene ontology terms identified by annotation. The author identified 749 biological process gene ontology terms enriched with the highly expressed genes, and the most significant enrichment was identified in terms related to immune response processes. Regarding cellular component gene ontology terms, cell membrane- or immunoglobulin-related pathways were the primary pathways enriched with the highly expressed genes.

The expression levels of the representative genes included in the gene ontology annotations in each sample are presented in Figure 9.

Figure 9. Representative gene expression levels.

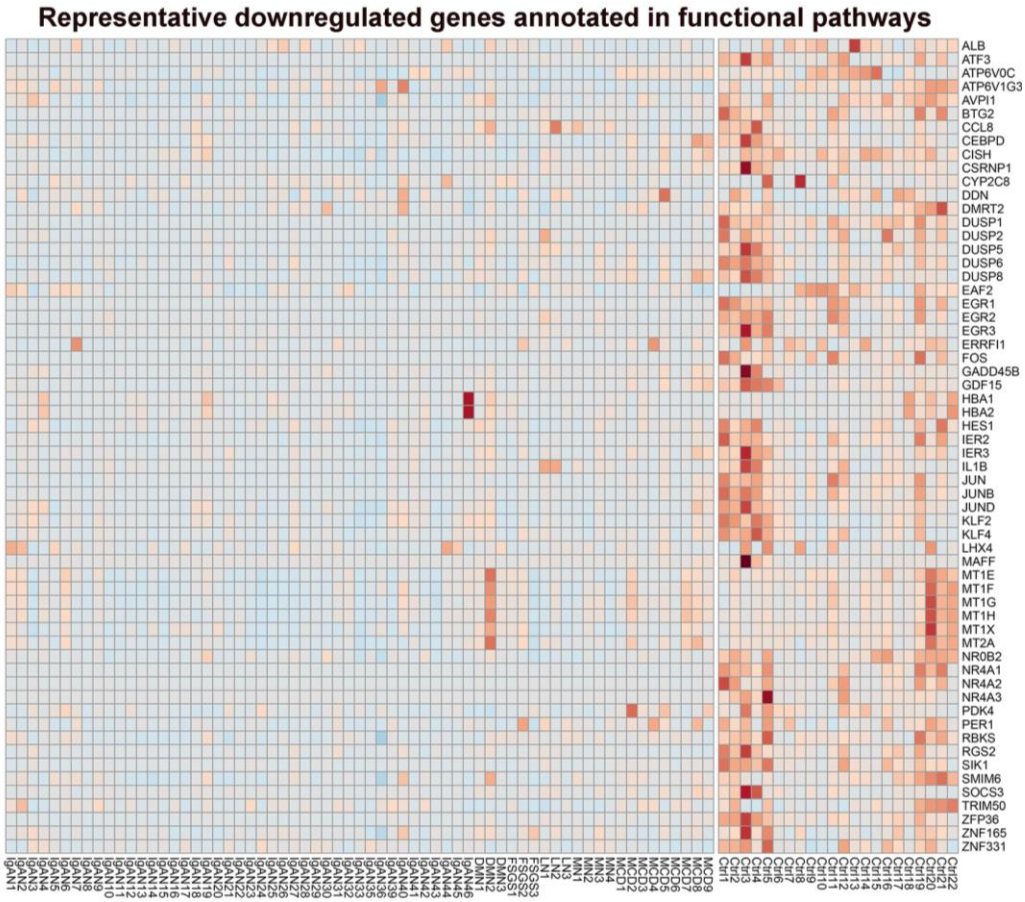

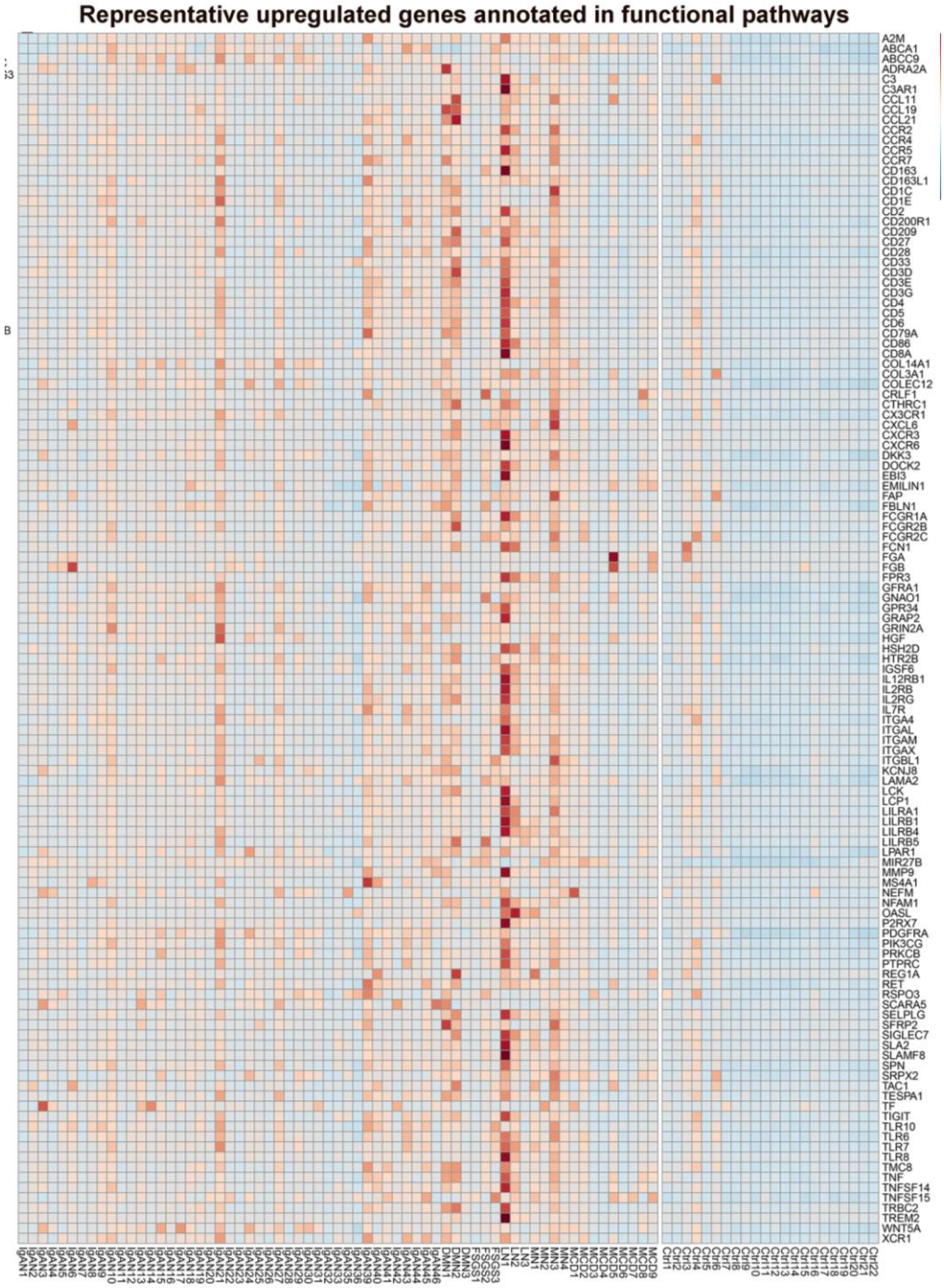

Representative gene expression levels in each sample. The plotted genes were annotated by gene ontology analysis. Red indicates relatively high expression, and blue indicates relatively low expression, graded in 10 ordinal categories. The representative genes were selected based on the gene ontology term annotation findings and the genes that most commonly annotated are presented in the figure.

4.5. Comparison with the IgAN-glomerular transcriptome

We compared the list of DEGs with those identified from the above IgAN glomerular RNA-seq, although some differences in disease categories or significance threshold were present (Table 5). Based on fold changes on the tubulointerstitial RNA-seq, the top 5 upregulated genes commonly identified in the tubulointerstitial and glomerular RNA-seq experiments were matrix metallopeptidase 9 (*MMP9*), CCR2, SLAM family member 7 (*SLAMF7*), leukocyte immunoglobulin-like receptor subfamily B member 4 (*LILRB4*), and immunoglobulin superfamily member 6 (*IGSF6*). On the other hand, the top 5 commonly downregulated genes included *FOS, EGR1, DUSP1*, activating transcription factor 3 (*ATF3*), and *JUNB*.

When we further inspected the upregulated DEGs, *IGHV* genes were identified as DEGs in tubulointerstitial RNA-seq but not in IgAN glomerular transcriptome. Otherwise, certain inflammatory DEGs (e.g. *CCL3, CCL4*) were only identified as DEGs in the glomerular RNA-seq of IgAN.

The downregulated DEGs only identified in the

tubulointerstitial RNA-seq included *NR4A1, NR4A2, NR4A3, RGS1,* and *EGR2*. Whilst *FOSB*, dual oxidase 2 (*DUOX2*), dynein axonemal heavy chain 2 (*DNAH2*), and myosin XVA (*MYO15A*) were the downregulated DEGs only identified in the glomerular RNA-seq of IgAN but not in the tubulointerstitial transcriptomic analysis results.

Table 5. Identification of top DEGs based on fold changes by comparison of glomerular and tubulointerstitial RNA-seq results.

List	Genes	Log2 fold changes	False-discovery rate
Commonly upregulated	*MMP9*	2.05	1.53E-06
	CCR2	1.80	2.19E-12
	SLAMF7	1.77	8.55E-09
	LILRB4	1.69	3.11E-10
	IGSF6	1.61	3.60E-13
Commonly downregulated	*FOS*	-5.92	9.76E-96
	EGR1	-4.34	5.28E-65
	DUSP1	-3.87	7.03E-132
	ATF3	-3.41	2.51E-42
	JUNB	-2.97	2.47E-24
Upregulated only in glomerular RNA-seq of IgAN	*CCL4*	3.39	3.15E-05
	CCL3	3.37	4.59E-05
	CD300C	3.09	2.66E-06
	APOBEC3A	2.83	1.77E-04
	SELE	2.82	3.29E-04
Downregulated only in glomerular RNA-seq of IgAN	*FOSB*	-4.36	3.93E-07
	AC099489.1	-3.73	3.90E-07
	DUOX2	-3.58	9.68E-06
	DNAH2	-3.57	8.19E-09
	MYO15A	-3.38	2.78E-08
Upregulated only in tubulointerstitial RNA-seq of various glomerulonephritis	*IGHV4-39*	3.04	1.51E-09
	IGHV1-18	2.82	1.93E-08
	IGHV3-23	2.78	2.70E-08
	IGHV3-15	2.71	2.25E-08
	IGHV2-5	2.67	1.04E-07
Downregulated only in tubulointerstitial RNA-seq of various glomerulonephritis	*NR4A1*	-4.79	3.14E-94
	NR4A2	-4.67	4.07E-85
	NR4A3	-4.45	6.34E-50
	RGS1	-3.13	1.43E-19
	EGR2	-2.82	1.30E-16

Commonly identified DEGs were selected from the statistical results in the tubulointerstitial RNA-seq.

4.6. Selection of the target gene

For further experimental validation, the author selected *DUSP1* as the target gene of interest, considering its significance level in our DEG analysis results (P = 7.03E-132, log 2-fold change -3.87). In addition, *DUSP1* appeared in a large proportion of the gene ontology annotation results (10/33 molecular function terms, 81/215 biological process terms), and the MAP kinase pathway, which is the direct target of *DUSP1*, was notably identified to be significantly downregulated in the profiled diseased kidney tubulointerstitial tissues.

When the author assessed the expression of *DUSP1* according to specific kidney disease types, all categories of profiled diseases showed significantly lower expression of *DUSP1* than the nephrectomy controls (Figure 10).

Figure 10. DUSP1 read counts in the study samples.

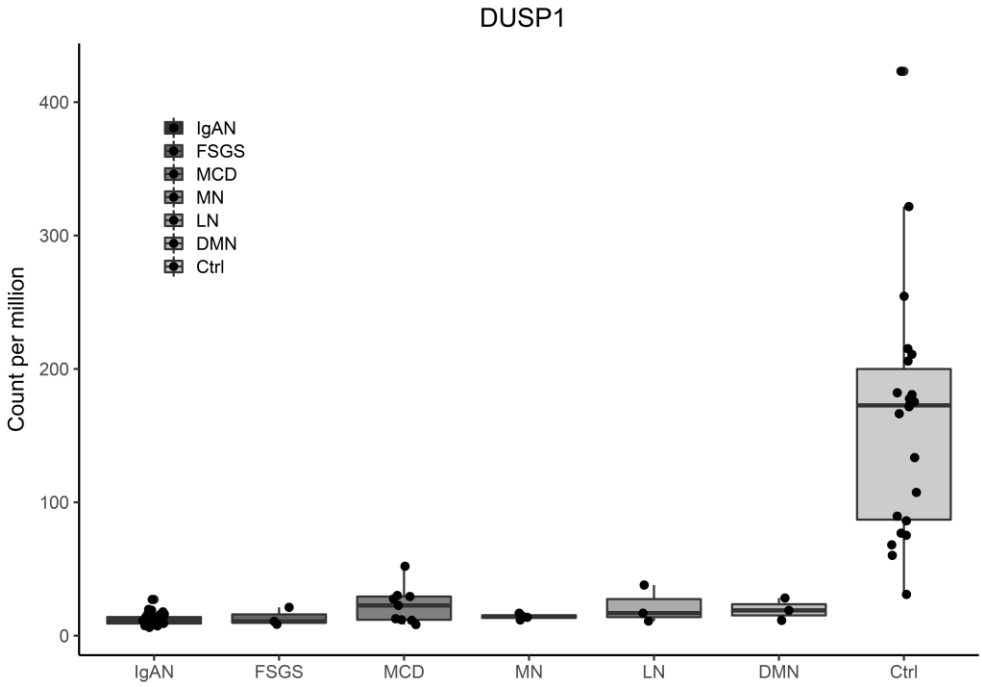

4.7. Immunohistochemical and immunofluorescence staining

Immunohistochemical staining of samples from patients with IgAN, membranous nephropathy, or minimal change disease and samples from nephrectomy controls indicated that the protein expression level of DUSP1 was significantly lower in the IgAN and membranous nephropathy samples than in the nephrectomy control samples (Figure 11A). However, in samples from patients with minimal change disease, no apparent difference was observed.

Immunofluorescence staining revealed similar findings, as DUSP1 expression was prominently reduced in samples from patients with IgAN or membranous nephropathy, while samples from patients with minimal change disease showed protein expression levels similar to those in samples from controls (Figure 11B).

When downstream molecules were assessed, expression of phospho-p38 was significantly higher in IgAN samples than in control cases (Figure 11A), but this pattern was not observed for minimal change disease or membranous nephropathy.

Expression of phosphor-ERK was significantly higher in glomerulonephritis cases than in controls, particularly for IgAN samples (Figure 11B).

Figure 11. Immunohistochemical and immunofluorescence staining results for DUSP1.

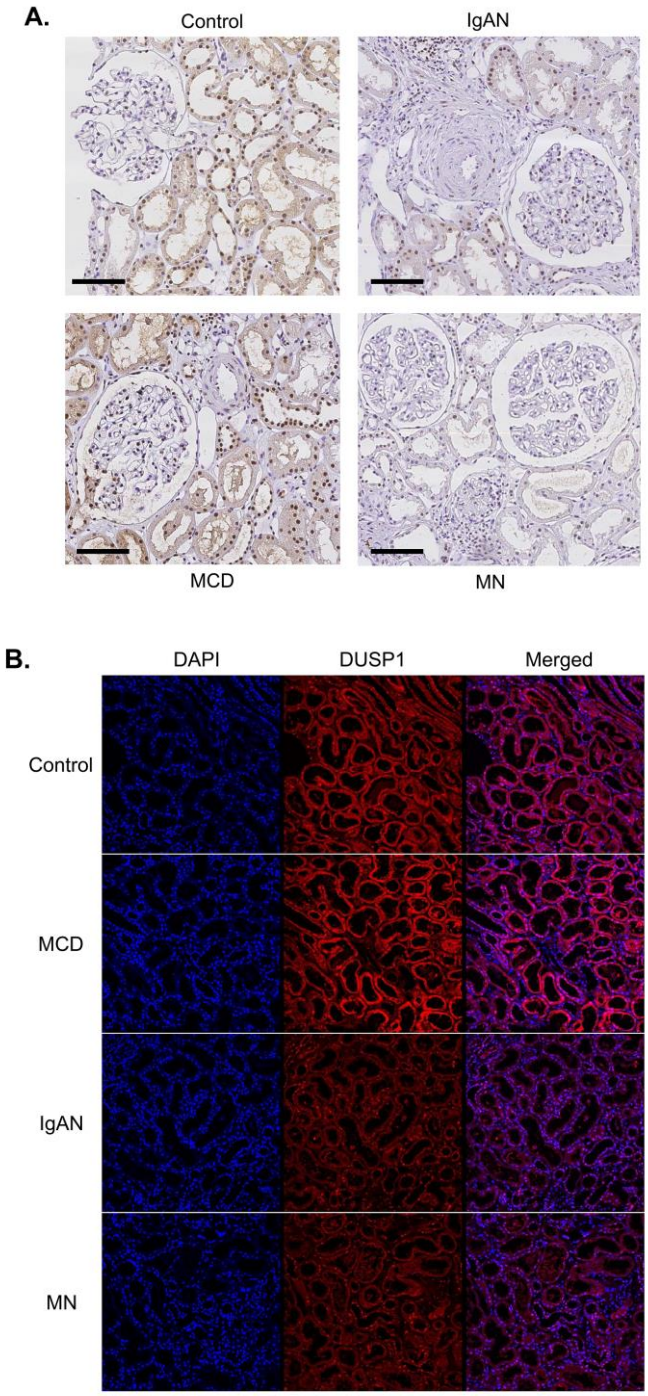

C.

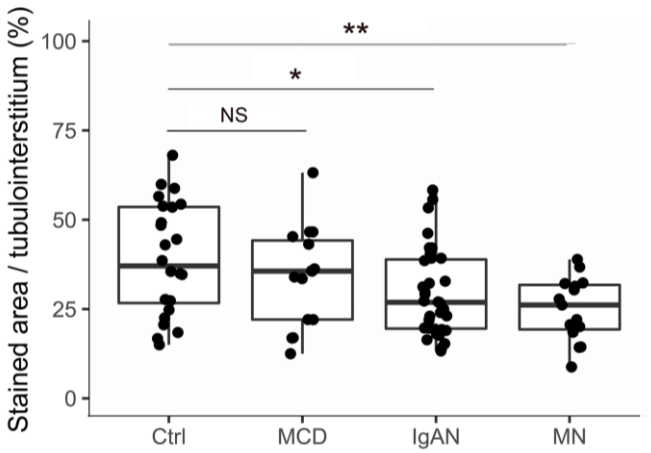

A: Representative immunohistochemical staining results for DUSP1 in samples from controls and patients with IgAN, minimal change disease (MCD), or membranous nephropathy (MN). The expression of DUSP1 was significantly lower in IgA nephropathy and membranous nephropathy samples than in control samples, but this pattern was not observed for minimal change disease samples. “NS” indicates a nonsignificant difference, “*” indicates $P < 0.05$, “**” indicates $P < 0.01$, and “***” indicates $P < 0.001$. B: Immunofluorescence staining showed findings similar to those of immunohistochemical staining, as the expression of DUSP1 was markedly lower in IgA nephropathy and membranous nephropathy samples than in control samples.

4.8. *In vitro* experimental results

The author further assessed markers of inflammation-related mechanisms associated with the MAP kinase pathway, including the expression of JNK, ERK, JUN, FOS, and AP1 along with modification of DUSP1.

Pharmacologic inhibition of DUSP1/6 with 5 mM BCI (Figure 12) was significantly associated with an increase in the level of phospho-p38. However, as BCI is an allosteric inhibitor, the expression level of DUSP1 changed only minimally with the addition of BCI. When the author evaluated the effect of BCI under various conditions (Figure 13), the effects of DUSP1/6 inhibition with BCI alone on the induction of target inflammatory molecules were similar to those of TNFα stimulation. When TNFα stimulation followed BCI treatment, the levels of phospho-JNK, phospho-ERK, phospho-FOS, and phospho-AP1 were further increased.

Figure 12. Experiment to determine the dosage of BCI treatment.

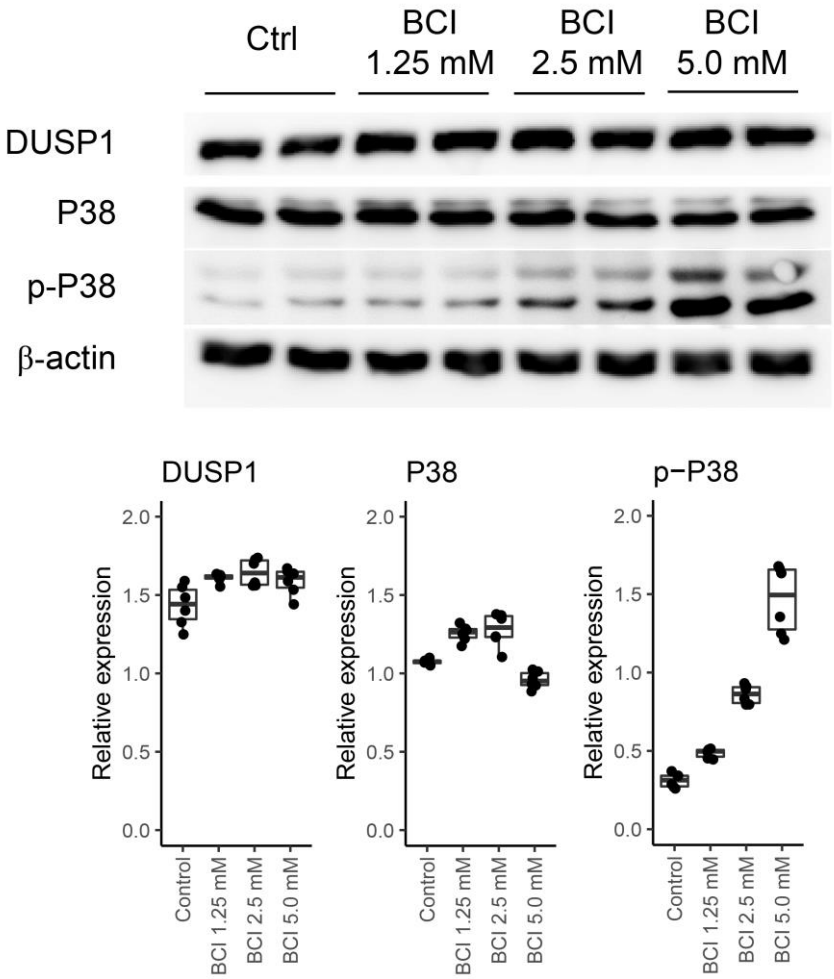

The author performed the experiment by adding BCI at 1.25 mM, 2.5 mM, and 5.0 mM to the culture medium of hTECs for 3 hours and then stimulating the hTECs with TNFα. The BCI concentration 5.0 mM was considered to sufficiently increase p38 expression was used for the main experiment.

Figure 13. *In vitro* western blot results for inhibition of DUSP1.

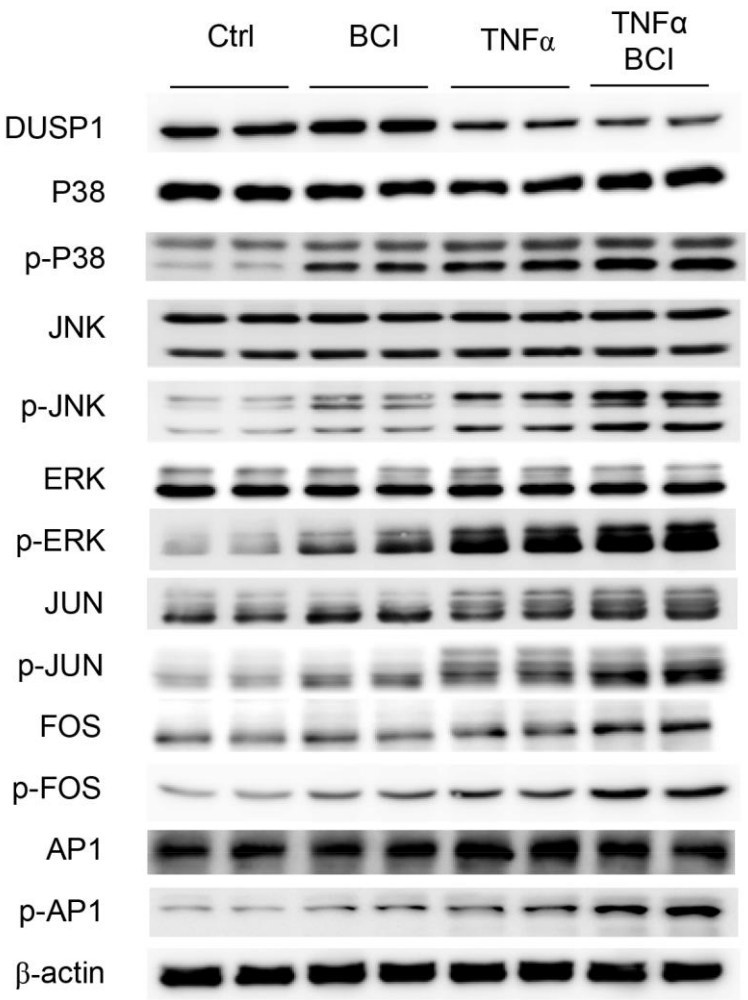

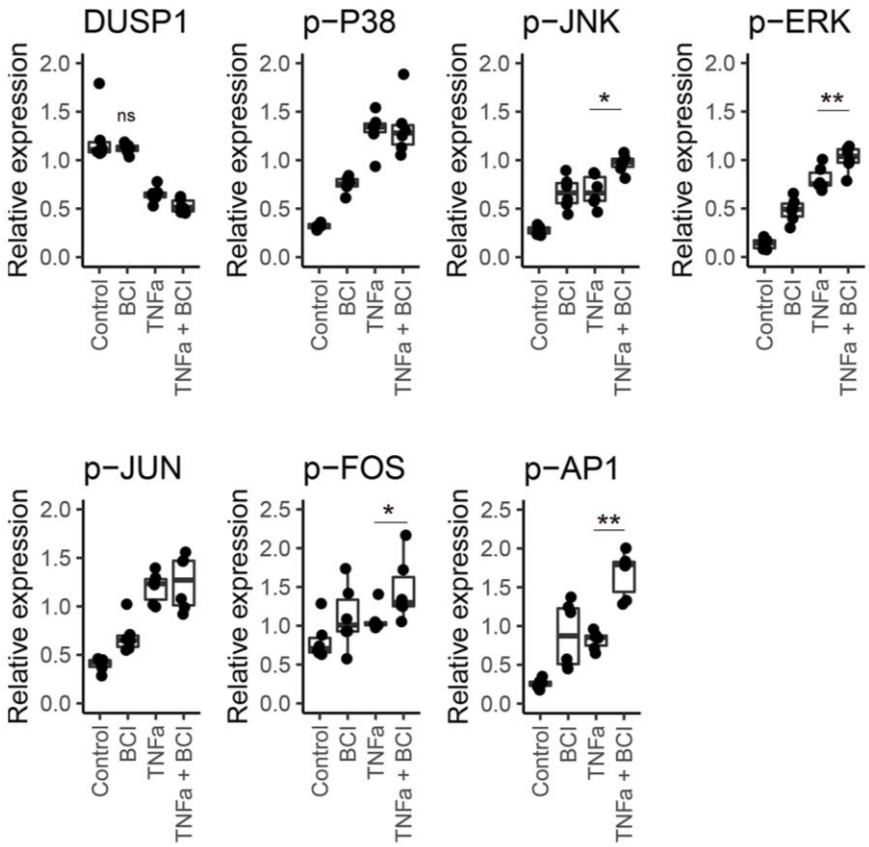

DUSP1 and inflammatory molecules in untreated hTECs, hTECs treated with 5.0 mM BCI for 3 hours, hTECs stimulated with 10 ng/mL TNFα for 1 hour, and hTECs treated with BCI and then stimulated with TNFα were analyzed by western blotting. All experiments were performed in triplicate. “ns” indicates a nonsignificant difference, “*” indicates $P < 0.05$, “**” indicates $P < 0.01$, and “***” indicates $P < 0.001$. When comparisons were performed with groups other than the control group, lines were drawn to indicate the groups that were compared.

On the other hand, adenovirus-mediated *DUSP1* overexpression at an MOI of 50, which was considered to induce sufficient *DUSP1* overexpression (Figure 14), reduced the levels of phospho-p38, phospho-JNK, and phospho-ERK compared to those in hTECs transduced with control adenovirus (Figure 15). Furthermore, when hTECs were transduced with adeno-*DUSP1* and stimulated with TNFα, the levels of most inflammatory molecules were markedly reduced compared to those in hTECs stimulated with TNFα alone.

Figure 14. Experiment to investigate the appropriate MOI of adeno-DUSP1 for DUSP1 overexpression.

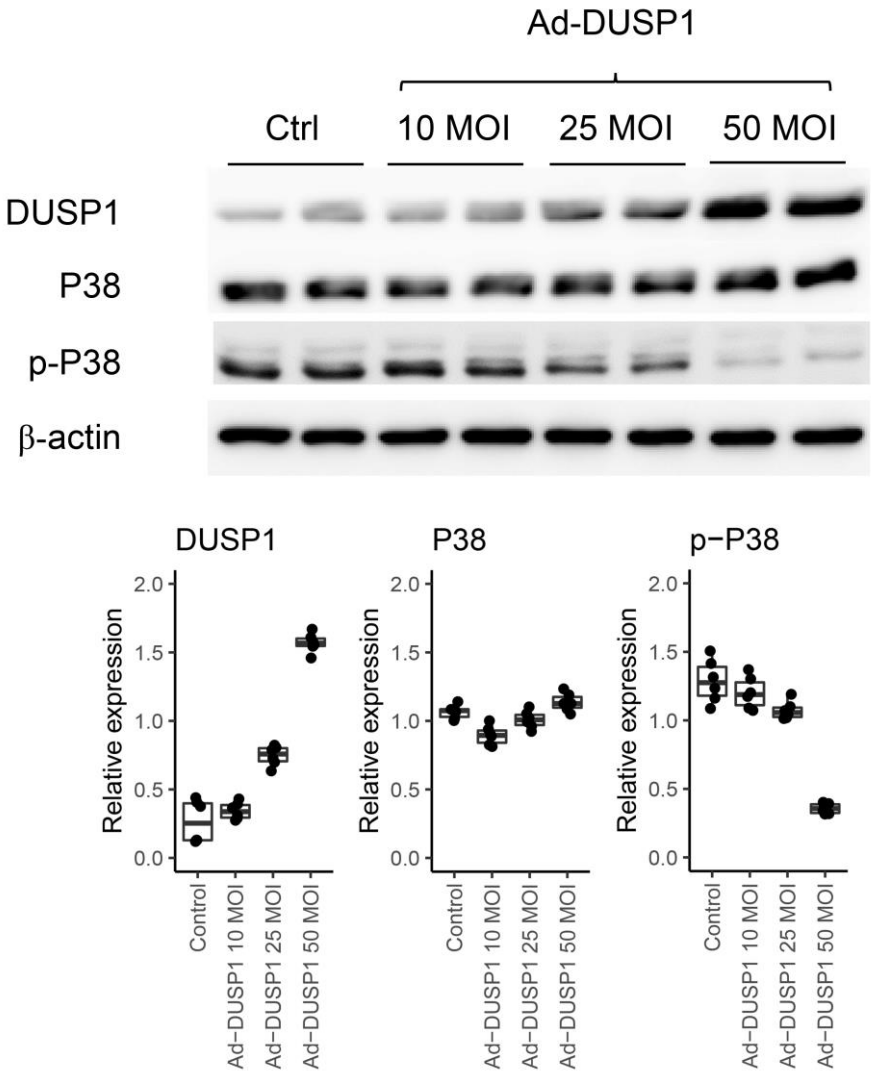

The author confirmed the appropriate multiplicity of infection (MOI) for DUSP1 overexpression by transducing cells with adeno-DUSP1 at MOIs of 10, 25, and 50 for 24 hours and assessing phospho-p38 and DUSP1 levels.

Figure 15. *In vitro* western blot results for DUSP1 overexpression.

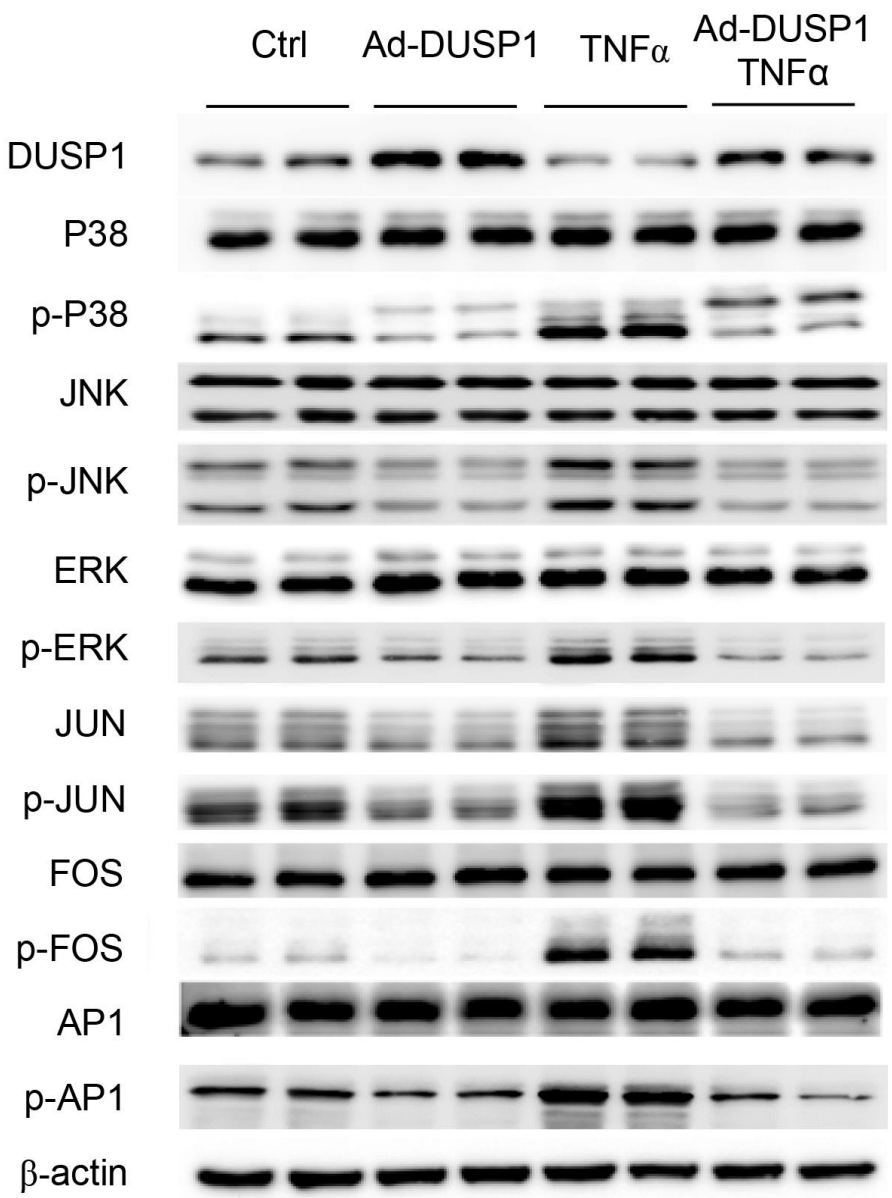

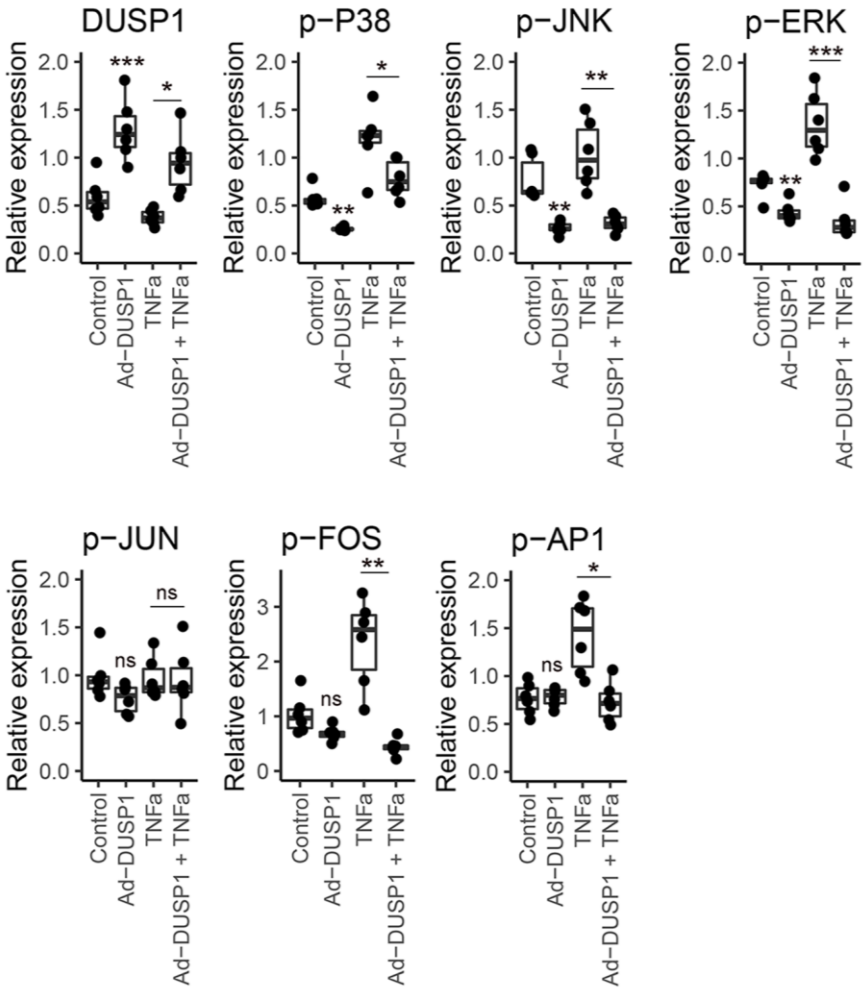

The experiment was performed in hTECs transfected with control adenovirus, hTECs transduced with DUSP1-adenovirus at 50 MOI, hTECs stimulated with TNFα, and hTECs transduced with DUSP1-adenovirus and then stimulated with TNFα. All experiments were performed in triplicate. “ns” indicates a nonsignificant difference, “*” indicates $P < 0.05$, “**” indicates $P < 0.01$, and “***” indicates $P < 0.001$. When comparisons were performed with groups other than the control group, lines were drawn to indicate the groups that were compared.

The author further aimed to assess whether modification of DUSP1 may be a potential corticosteroid-preserving anti-inflammatory strategy by comparing the effects of DUSP1 overexpression and dexamethasone treatment on stimulated hTECs. In the experiment to determine the appropriate corticosteroid concentration, treatment with a low concentration (0.25 mM, Figure 16) of dexamethasone did not result in significant reductions in the levels of phospho-p38, phospho-JNK, and phospho-ERK or a change in DUSP1 expression but did decrease the levels of phospho-JUN, phospho-FOS, and phospho-AP1 (Figure 17). In contrast, treatment with a high concentration (1.0 mM) of dexamethasone decreased the levels of certain inflammatory molecules and increased the expression of DUSP1. When hTECs overexpressing DUSP1 were treated with 0.25 mM dexamethasone, the DUSP1 expression level was similar to that in hTECs treated with the high concentration of dexamethasone, and the levels of the target inflammatory molecules were significantly reduced even compared those after 1.0 mM dexamethasone treatment.

Figure 16. Experiment to investigate dexamethasone dosage.

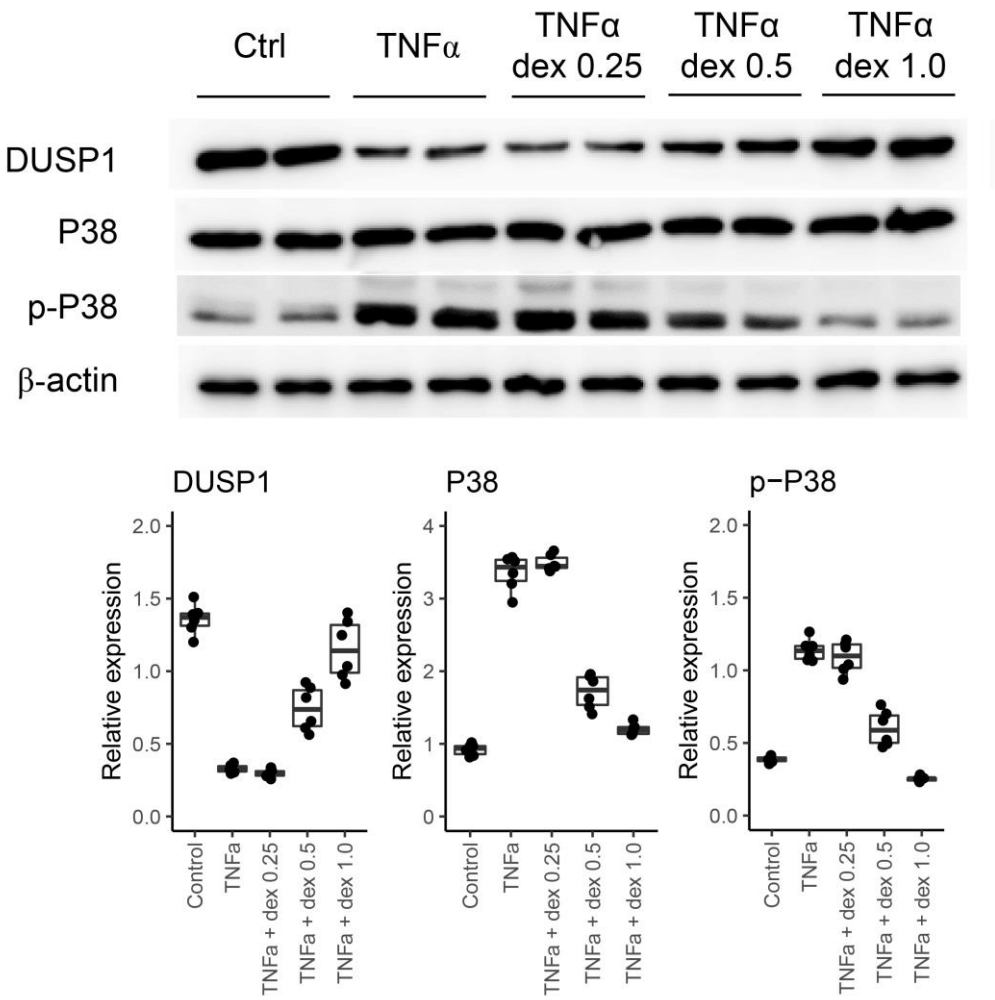

The author assessed phospho-p38 and DUSP1 levels in hTECs treated with 0.25, 0.5, and 1.0 mM dexamethasone for 1 hour and then stimulated with TNFα.

Figure 17. *In vitro* western blot results for DUSP1 overexpression with addition of corticosteroid treatment.

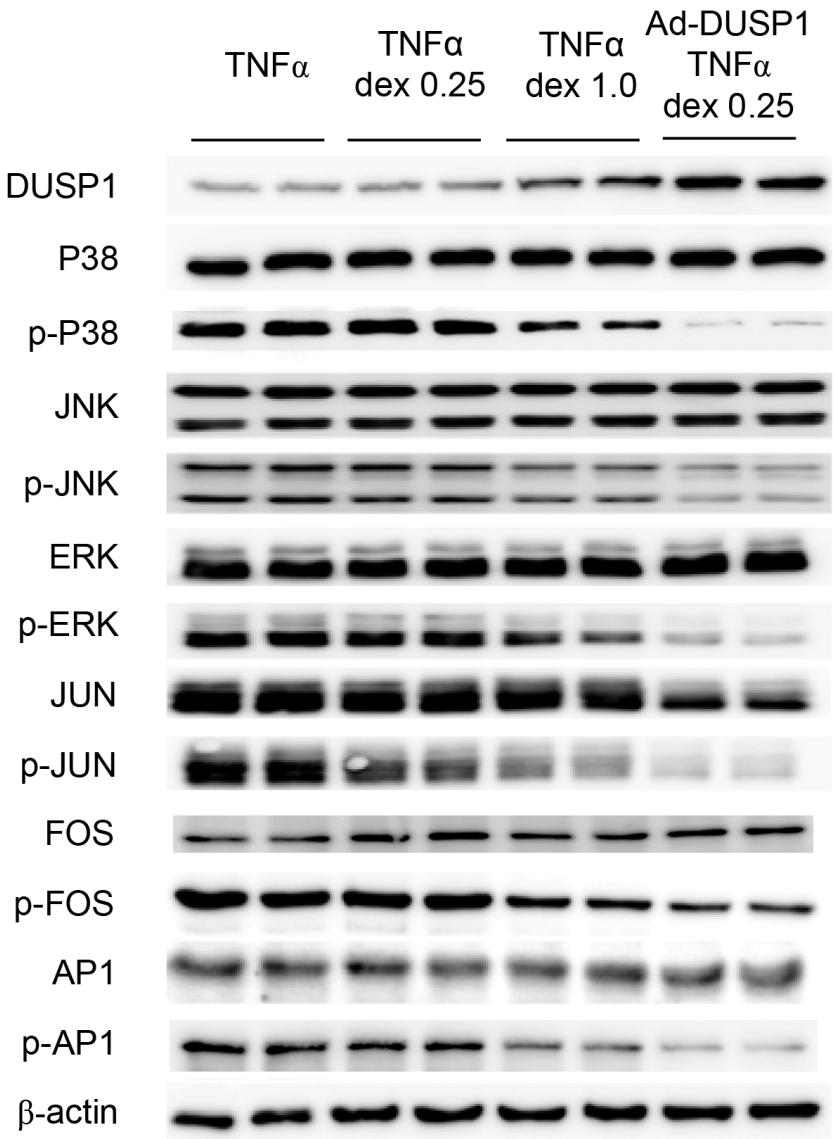

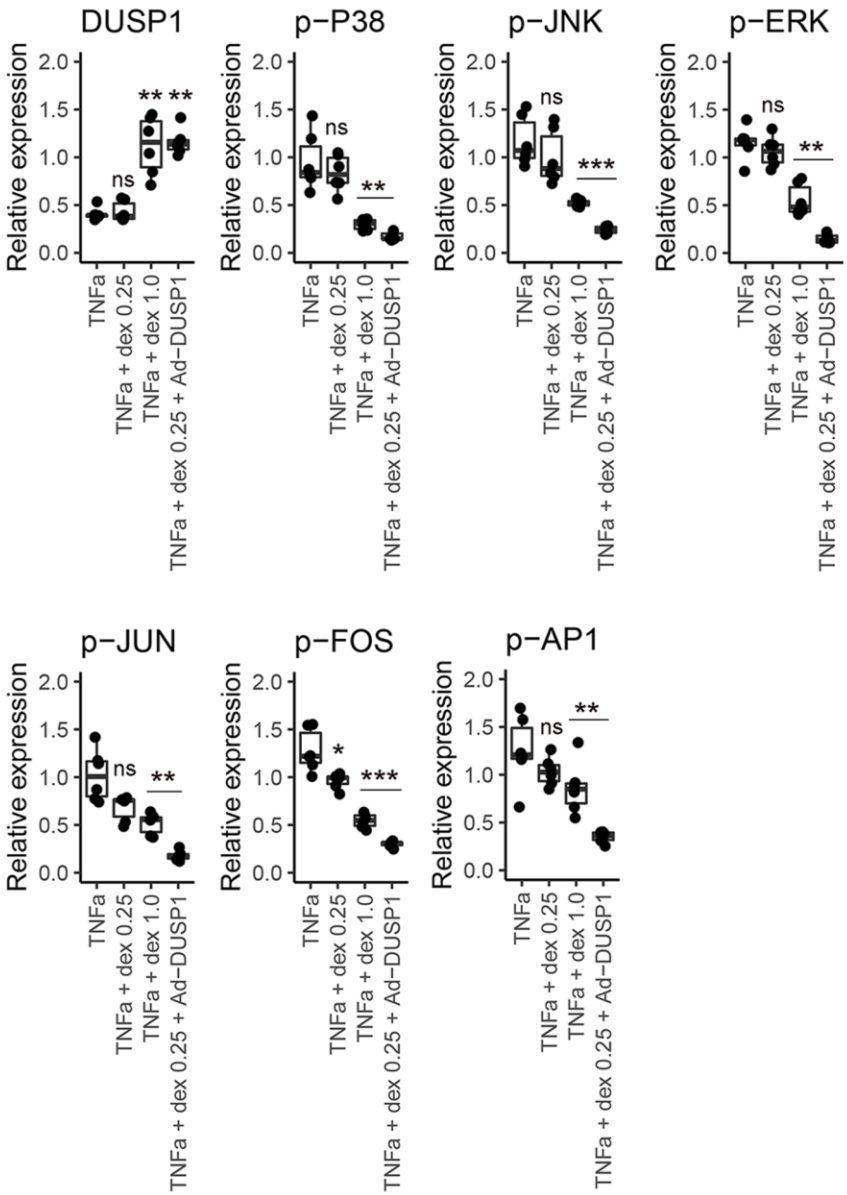

The experiment was performed in hTECs transduced with control adenovirus and stimulated with TNFα, in control adenovirus-transduced hTECs stimulated with TNFα and treated with dexamethasone (0.25 mM), in control adenovirus-transduced hTECs stimulated with TNFα and treated with dexamethasone (1.0 mM), and in DUSP1-adenovirus-transduced hTECs stimulated with TNFα and treated with dexamethasone (0.25 mM). All experiments were performed in triplicate. “ns” indicates a nonsignificant difference, “*” indicates $P < 0.05$, “**” indicates $P < 0.01$, and “***” indicates $P < 0.001$. When comparisons were performed with groups other than the control group, lines were drawn to indicate the groups that were compared.

Chapter 5. Discussion

The author performed RNA-seq in glomerulus and transcriptomic tissue of glomerulonephritis. The transcriptomic profile identified distinct differences in diverse forms of glomerulonephritis when compared to nephrectomy controls in kidney substructure. The author found some notable inflammation pathway-related DEGs are commonly downregulated in the glomerulus of IgAN and tubulointerstitial tissue of glomerulonephritis (e.g. *DUSP1, FOS*, and *EGR1*). On the other hand, certain DEGs (e.g. *CCL3 and CCL4* in IgAN glomerulus RNA-seq, and *IGHV* and *NR4A* genes in tubulointerstitial RNA-seq) were only identified in the analysis of the specific kidney substructure. The results suggested that certain gene expressions may be similarly altered in glomerulonephritis both in glomerulus and tubulointerstitial tissue reflecting the global inflammatory aspects of a total kidney. However, the pathophysiologic mechanism of glomerulonephritis is commonly explained by glomerular-

tubulointerstitial crosstalk. Although the exact sequences of alteration of gene expressions in glomerulus and tubulointerstitial tissue need additional investigation, the current RNA-seq experiment suggests that RNA-seq of kidney substructure can identify distinct RNA changes in glomerulus or tubulointerstitial tissue, providing insights related to structure-specific pathophysiologic mechanisms of glomerulonephritis. Future research implementing advanced RNA-seq technology with spatial information may be used to reveal gene expression profiles of detailed kidney substructures expanding the current knowledge of glomerular-tubulointerstitial mechanism of diverse glomerulonephritis.

5.1. Findings in IgAN glomerulus RNA-seq

In the glomerulus RNA-seq for IgAN, differential-expression analysis and pathway enrichment analysis revealed that molecular pathways associated with B cell functions, chemokines, inflammation, and Fcɣ receptors were significantly enriched in the glomeruli from IgAN transcriptome. Among the genes upregulated in IgAN was *SYK*, whose

biological role in IgAN has been previously reported.[15] Our *in vitro* experiment with a primary culture of mesangial cells and patient-derived sera or IgA1 extracts was consistent with the findings from RNA-seq profiling, further supporting the potential role of this kinase in the pathogenesis of IgAN.

While the production of galactose-deficient IgA molecules and their deposition in the mesangium is essential in the pathogenesis of IgAN,[30,31] its significance in the progression of IgAN remains mostly unknown, leaving an unmet need for a disease-specific biomarker or treatment target in IgAN.[28] Although a multi-hit hypothesis has been proposed regarding IgAN, a study on the final step of the suggested pathophysiology was warranted.[32,33] To investigate the pathophysiology related to glomerular injury, a lot of effort has been made to demonstrate the molecular mechanisms in IgAN glomeruli. Profiling IgAN patients with the comparable renal function was necessary, preferably with those without significant kidney function impairment since chronic kidney disease itself alters the glomerular transcriptome.[2,34,35] A major strength of our study is that the author profiled the

transcriptome of microdissected IgAN glomeruli using the RNA-seq technique, including a homogeneous patient group with preserved kidney function. The author attempted a novel methodology of intra-glomerular pathogenesis investigation as well as suggested the potential molecules and pathways related to the IgAN before reaching profound kidney dysfunction.

Several reported expressed genes regarding IgAN development or the disease activity were again confirmed to be differentially expressed in IgAN glomeruli. Chemokine-chemokine receptor pathways were reported to be important chemokines related to inflammatory glomerulonephritis, including IgAN.[36-38] Although the overexpression of chemokines is not specific to the pathogenesis of IgAN, our result suggested the inflammatory pathways play a significant role in the IgAN glomeruli even before profound kidney dysfunction develops. For example, *CX3CR1*, a gene encoding for the chemokine receptor related to homing of inflammatory cells, was reported to be overexpressed during a bout of gross hematuria in IgAN.[39,40] Consistent with these prior reports, our transcriptomic profiling showed that *CX3CR1* transcripts were

highly expressed in the IgAN glomeruli. Phosphoinositide 3-kinase, a downstream molecule of significantly overexpressed pathways including B cell signaling or chemokine signaling pathways, is related to podocyte injury of IgAN.[41,42] The author also found that a recently proposed mesangial cell receptor for IgA, namely *B4GALT1,* but not transferrin receptor (*CD71*), was upregulated in the transcriptome of IgAN, further supporting its importance in IgAN pathophysiology.[43] As previously reported, *AGTR1*, one of the target molecules of commonly implemented renin-angiotensin-aldosterone system blockade therapy, was downregulated in IgAN glomerular transcriptome.[27]

The pathway enrichment analysis showed that inflammation-related pathways, similarly as individual gene expression results, were highly expressed in glomeruli of IgAN patients with relatively preserved kidney function. MAPK, PI3K-Akt, NF-kB signaling pathways, which were important inflammation-related pathways, were shared among the identified KEGG pathway analysis results, and the most frequently identified pathway was the MAPK signaling pathway.

The MAPK signaling pathway was reported to be an important pathophysiologic mechanism of IgAN and is related to renin-angiotensin system activity, which is the current main potential therapeutic target for the disease.[44] Also, PI3K-Akt pathway has been reported to be overexpressed in IgAN patients.[42] The Fcɣ receptor-mediated phagocytosis might be related to the role of inflammatory phagocytosis or innate immunity in IgAN development.[45] Therefore, the molecules identified in our pathway analysis, particularly those related to inflammation, can be targets for future development of diagnostic or therapeutic measures for IgAN.

Of the DEGs identified in our study, the author chose to confirm the intraglomerular expression of SYK. The pathophysiologic significance of SYK has been highlighted in IgAN, and there is an ongoing clinical trial of fostamatinib, a molecularly targeting agent against SYK for patients with IgAN.[28,29,46] In addition, another pre-clinical study showed that SYK inhibition improved crescentic glomerulonephritis in animal models.[47] Although the expression of SYK was not highly prominent in glomerulus of IgAN with our

immunohistochemistry staining of IgAN patients without significantly reduced eGFR or nephrotic range proteinuria, cases of IgAN with reduced eGFR (< 60 mL/min/1.73m^2) exhibited clearly upregulated expression of phospho-SYK in their glomeruli. Based on the high sensitivity of RNA-seq results, the author believe that SYK can be considered a potential "druggable" target in IgAN with preserved kidney function, although SYK expression in early IgAN specimens was not detected on immunohistochemistry.

5.2. Findings in tubulointerstitial RNA-seq for various glomerulonephritis

In the tubulointerstitial RNA-seq, the expression levels of various genes were altered in the diseased tubulointerstitium compared to the normal cortex, and the activity of relevant inflammation-related pathways was altered. Among the DEGs, the author performed experimental studies with *DUSP1*, which was universally expressed at low levels in injured kidney tubulointerstitial tissues in various kidney diseases. The results suggested that modification of *DUSP1* expression is a potential

therapeutic strategy for renal tubulointerstitial injury.

Based on the pathway annotation results and false discovery rates, *DUSP1*, which downregulates the MAP kinase pathway, was selected as the target biomarker for further validation. Activation of the MAP kinase pathway is a core mechanism mediating various glomerulonephritis.[48-51] In our study, the expression of *DUSP1* was generally reduced in various types of glomerulonephritis, which may promote upregulation of the MAP kinase pathway and related inflammatory signaling. The role of *DUSP1* has been suggested in few studies regarding kidney diseases, although previous experimental studies reported that *DUSP1* ameliorates diabetic kidney diseases.[52,53] As both downregulation and upregulation of DUSP1 resulted in altered inflammatory signaling activity in our study, DUSP1 in the kidney tubulointerstitium may be a potential target to reduce inflammation and tubulointerstitial injury.

The promoter region of the *DUSP1* gene contains binding sites for AP1, nuclear factor-κB, cAMP response element-binding protein, and glucocorticoid receptor. Previous studies have focused on the observation that the effects of glucocorticoids

are mediated by *DUSP1*, as the binding of glucocorticoids to glucocorticoid receptors induces *DUSP1* transcription, which is the major mechanism further downregulating inflammatory pathways.[54] In particular, the role of *DUSP1* has been emphasized in airway inflammatory diseases (e.g., asthma or chronic obstructive pulmonary diseases), where glucocorticoids are the primary choice of treatment for acute exacerbated states.[55] As targeting *DUSP1* has shown anti-inflammatory effects in airway cells and *in vivo* models, *DUSP1* has been suggested to be a potential therapeutic target for steroid-resistant cases.[56-58] Regarding glomerulonephritis, glucocorticoids are also a widely used treatment strategy for various inflammation-related conditions. Glucocorticoids have limitations because of side effects due to their broad effect on diverse systems; thus, modification of *DUSP1* expression may be an alternative treatment strategy with limited use of steroids, as suggested by our *in vitro* experimental results. This strategy would be particularly important in diabetic kidney diseases, in which the role of *DUSP1* has also been identified by *in vivo* experiments,[53] and direct modification of *DUSP1* may reduce

inflammatory injury while avoiding the metabolic side effects of glucocorticoids. Alternatively, for glomerulonephritis for which glucocorticoid treatment has limited efficacy, directly targeting *DUSP1* may be a potential strategy to prevent tubulointerstitial injury because of its potency. Thus, the results of our study support future studies to test the efficacy of targeting *DUSP1* in various glomerulonephritis and researchers may particularly focus on the validation of the benefits of *DUSP1* restoration by *in vivo* experiments.

5.3. Limitations

The current study leaves several limitations and questions that need to be addressed in future studies. First, as microdissected tissue is still a bulk tissue consisting several cell types, identification of the cell-specific transcriptome was not performed herein. However, although single-cell sequencing technology can help delineate transcriptomic changes occurring in individual cells, human kidney tissues obtained from kidney biopsies are not usually conducive to direct preparation for single-cell study mainly due to limited

number of glomeruli and large amounts of blood cell contamination in the biopsy core. Third, although the microstructure-specific transcriptomic profiling was performed, whether the findings reflect certain pathologic readings remains to be resolved. For instance, glomerulus in IgAN exhibit diverse pathologic changes (e.g. mesangial proliferation, segmental sclerosis) and the findings may be different according to such status. Therefore, additional study incorporating spatial transcriptomic profiling strategy may be warranted to further dissect the transcriptomic profiles of glomerulonephritis. Lastly, our study subjects were all East Asians, so ethnic differences need to be considered for generalization of our study results.

5.4. Conclusions

In conclusion, transcriptome profiling of glomerulus and tubulointerstitial tissue in patients with various glomerulonephritis revealed notable findings that may provide insights into pathophysiologic mechanisms. Future studies may consider the clinical implementation of the identified

biomarkers and test whether the modification of the targets may be helpful in treatment of glomerulonephritis.

Bibliography

1. Global, regional, and national burden of chronic kidney disease, 1990-2017: a systematic analysis for the Global Burden of Disease Study 2017. *Lancet.* 2020;395:709-733.
2. Craciun FL, Bijol V, Ajay AK, et al. RNA Sequencing Identifies Novel Translational Biomarkers of Kidney Fibrosis. *J Am Soc Nephrol.* 2016;27:1702-1713.
3. Park S, Yang SH, Jeong CW, et al. RNA-Seq profiling of microdissected glomeruli identifies potential biomarkers for human IgA nephropathy. *Am J Physiol Renal Physiol.* 2020;319:F809-f821.
4. Park S, Lee H, Lee J, et al. RNA-seq profiling of tubulointerstitial tissue reveals a potential therapeutic role of dual anti-phosphatase 1 in glomerulonephritis. *J Cell Mol Med.* 2022;26:3364-3377.
5. Martin M. Cutadapt removes adapter sequences from high-throughput sequencing reads. *EMBnetjournal.* 2011;17:10-12.
6. Langmead B, Salzberg SL. Fast gapped-read alignment

with Bowtie 2. *Nat Methods.* 2012;9:357-359.

7. Liao Y, Smyth GK, Shi W. featureCounts: an efficient general purpose program for assigning sequence reads to genomic features. *Bioinformatics.* 2014;30:923-930.

8. Anders S, Pyl PT, Huber W. HTSeq--a Python framework to work with high-throughput sequencing data. *Bioinformatics.* 2015;31:166-169.

9. Lê S J, J, Husson F. FactoMineR: An R Package for Multivariate Analysis. *Journal of Statistical Software.* 2008;25:1-18.

10. Love MI, Huber W, Anders S. Moderated estimation of fold change and dispersion for RNA-seq data with DESeq2. *Genome Biol.* 2014;15:550.

11. Luo W, Brouwer C. Pathview: an R/Bioconductor package for pathway-based data integration and visualization. *Bioinformatics.* 2013;29:1830-1831.

12. Young MD, Wakefield MJ, Smyth GK, Oshlack A. Gene ontology analysis for RNA-seq: accounting for selection bias. *Genome Biol.* 2010;11:R14.

13. Chen J, Bardes EE, Aronow BJ, Jegga AG. ToppGene

Suite for gene list enrichment analysis and candidate gene prioritization. *Nucleic Acids Res.* 2009;37:W305-311.

14. Lee H, Lee JW, Yoo KD, et al. Cln 3-requiring 9 is a negative regulator of Th17 pathway-driven inflammation in anti-glomerular basement membrane glomerulonephritis. *Am J Physiol Renal Physiol.* 2016;311:F505-519.

15. Kim MJ, McDaid JP, McAdoo SP, et al. Spleen tyrosine kinase is important in the production of proinflammatory cytokines and cell proliferation in human mesangial cells following stimulation with IgA1 isolated from IgA nephropathy patients. *J Immunol.* 2012;189:3751-3758.

16. An JN, Yang SH, Kim YC, et al. Periostin induces kidney fibrosis after acute kidney injury via the p38 MAPK pathway. *Am J Physiol Renal Physiol.* 2019;316:F426-f437.

17. Jeffrey KL, Camps M, Rommel C, Mackay CR. Targeting dual-specificity phosphatases: manipulating MAP kinase signalling and immune responses. *Nat Rev Drug Discov.*

2007;6:391-403.

18. Ernandez T, Mayadas TN. Immunoregulatory role of TNFalpha in inflammatory kidney diseases. *Kidney Int.* 2009;76:262-276.

19. Chan LY, Leung JC, Tsang AW, et al. Activation of tubular epithelial cells by mesangial-derived TNF-alpha: glomerulotubular communication in IgA nephropathy. *Kidney Int.* 2005;67:602-612.

20. Sun L, Kanwar YS. Relevance of TNF-α in the context of other inflammatory cytokines in the progression of diabetic nephropathy. *Kidney Int.* 2015;88:662-665.

21. Molina G, Vogt A, Bakan A, et al. Zebrafish chemical screening reveals an inhibitor of Dusp6 that expands cardiac cell lineages. *Nat Chem Biol.* 2009;5:680-687.

22. Kesarwani M, Kincaid Z, Gomaa A, et al. Targeting c-FOS and DUSP1 abrogates intrinsic resistance to tyrosine-kinase inhibitor therapy in BCR-ABL-induced leukemia. *Nat Med.* 2017;23:472-482.

23. Kent WJ, Sugnet CW, Furey TS, et al. The human genome browser at UCSC. *Genome Res.* 2002;12:996-

1006.

24. Naga Prasad SV, Barak LS, Rapacciuolo A, et al. Agonist-dependent recruitment of phosphoinositide 3-kinase to the membrane by beta-adrenergic receptor kinase 1. A role in receptor sequestration. *J Biol Chem.* 2001;276:18953-18959.

25. Liu M, Ning X, Li R, et al. Signalling pathways involved in hypoxia-induced renal fibrosis. *J Cell Mol Med.* 2017;21:1248-1259.

26. Molyneux K, Wimbury D, Pawluczyk I, et al. beta1,4-galactosyltransferase 1 is a novel receptor for IgA in human mesangial cells. *Kidney Int.* 2017;92:1458-1468.

27. Lai KN, Chan LY, Tang SC, et al. Mesangial expression of angiotensin II receptor in IgA nephropathy and its regulation by polymeric IgA1. *Kidney Int.* 2004;66:1403-1416.

28. Ma TK, McAdoo SP, Tam FW. Targeting the tyrosine kinase signalling pathways for treatment of immune-mediated glomerulonephritis: from bench to bedside and beyond. *Nephrol Dial Transplant.* 2017;32:i129-i138.

29. Markham A. Fostamatinib: First Global Approval. *Drugs.* 2018;78:959-963.

30. Suzuki H, Fan R, Zhang Z, et al. Aberrantly glycosylated IgA1 in IgA nephropathy patients is recognized by IgG antibodies with restricted heterogeneity. *J Clin Invest.* 2009;119:1668-1677.

31. Suzuki H, Moldoveanu Z, Hall S, et al. IgA1-secreting cell lines from patients with IgA nephropathy produce aberrantly glycosylated IgA1. *J Clin Invest.* 2008;118:629-639.

32. Suzuki H, Kiryluk K, Novak J, et al. The pathophysiology of IgA nephropathy. *J Am Soc Nephrol.* 2011;22:1795-1803.

33. Kiryluk K, Novak J. The genetics and immunobiology of IgA nephropathy. *J Clin Invest.* 2014;124:2325-2332.

34. Kottgen A, Glazer NL, Dehghan A, et al. Multiple loci associated with indices of renal function and chronic kidney disease. *Nat Genet.* 2009;41:712-717.

35. Martini S, Nair V, Keller BJ, et al. Integrative biology identifies shared transcriptional networks in CKD. *J Am*

Soc Nephrol. 2014;25:2559-2572.

36. Gan L, Zhou Q, Li X, et al. Intrinsic renal cells induce lymphocytosis of Th22 cells from IgA nephropathy patients through B7-CTLA-4 and CCL-CCR pathways. *Mol Cell Biochem.* 2018;441:191-199.

37. Anders HJ, Vielhauer V, Kretzler M, et al. Chemokine and chemokine receptor expression during initiation and resolution of immune complex glomerulonephritis. *J Am Soc Nephrol.* 2001;12:919-931.

38. Vielhauer V, Berning E, Eis V, et al. CCR1 blockade reduces interstitial inflammation and fibrosis in mice with glomerulosclerosis and nephrotic syndrome. *Kidney Int.* 2004;66:2264-2278.

39. Cox SN, Sallustio F, Serino G, et al. Activated innate immunity and the involvement of CX3CR1-fractalkine in promoting hematuria in patients with IgA nephropathy. *Kidney Int.* 2012;82:548-560.

40. Batra A, Smith AC, Feehally J, Barratt J. T-cell homing receptor expression in IgA nephropathy. *Nephrol Dial Transplant.* 2007;22:2540-2548.

41. Wang C, Liu X, Ke Z, et al. Mesangial medium from IgA nephropathy patients induces podocyte epithelial-to-mesenchymal transition through activation of the phosphatidyl inositol-3-kinase/Akt signaling pathway. *Cell Physiol Biochem.* 2012;29:743-752.

42. Cox SN, Sallustio F, Serino G, et al. Altered modulation of WNT-beta-catenin and PI3K/Akt pathways in IgA nephropathy. *Kidney Int.* 2010;78:396-407.

43. Molyneux K, Wimbury D, Pawluczyk I, et al. β1,4-galactosyltransferase 1 is a novel receptor for IgA in human mesangial cells. *Kidney Int.* 2017;92:1458-1468.

44. Tamouza H, Chemouny JM, Raskova Kafkova L, et al. The IgA1 immune complex-mediated activation of the MAPK/ERK kinase pathway in mesangial cells is associated with glomerular damage in IgA nephropathy. *Kidney Int.* 2012;82:1284-1296.

45. Arima S, Nakayama M, Naito M, et al. Significance of mononuclear phagocytes in IgA nephropathy. *Kidney Int.* 1991;39:684-692.

46. F. Tam WK JT, J. Barratt, B. Rovin H, I. Roberts SD, C.

Roufosse, H.T. Cook, S. Tong, D. Magilavy, R. Lafayette. SUN-036 SPLEEN TYROSINE KINASE (SYK) INHIBITION IN IGA NEPHROPATHY: A GLOBAL, PHASE II, RANDOMISED PLACEBO-CONTROLLED TRIAL OF FOSTAMATINIB. *Kidney reports.* 2019;4:S168.

47. Stephen P. McAdoo MP, Anisha Tanna, Tejal Bhatt, Gurjeet Bhangal, John McDaid, Esteban S. Masuda, H. Terence Cook, Frederick WK. Tam, Charles D. Pusey. Spleen tyrosine kinase inhibition is an effective treatment for established vasculitis in a pre-clinical model. *Kidney Int.* 2020.

48. Stambe C, Atkins RC, Tesch GH, et al. The role of p38alpha mitogen-activated protein kinase activation in renal fibrosis. *J Am Soc Nephrol.* 2004;15:370-379.

49. Awazu M, Ishikura K, Hida M, Hoshiya M. Mechanisms of mitogen-activated protein kinase activation in experimental diabetes. *J Am Soc Nephrol.* 1999;10:738-745.

50. Ma FY, Tesch GH, Ozols E, et al. TGF-β1-activated kinase-1 regulates inflammation and fibrosis in the

obstructed kidney. *Am J Physiol Renal Physiol.* 2011;300:F1410-1421.

51. Lee J, An JN, Hwang JH, et al. p38 MAPK activity is associated with the histological degree of interstitial fibrosis in IgA nephropathy patients. *PLoS One.* 2019;14:e0213981.

52. Ge Y, Wang J, Wu D, et al. lncRNA NR_038323 Suppresses Renal Fibrosis in Diabetic Nephropathy by Targeting the miR-324-3p/DUSP1 Axis. *Mol Ther Nucleic Acids.* 2019;17:741-753.

53. Sheng J, Li H, Dai Q, et al. DUSP1 recuses diabetic nephropathy via repressing JNK-Mff-mitochondrial fission pathways. *J Cell Physiol.* 2019;234:3043-3057.

54. Hoppstädter J, Ammit AJ. Role of Dual-Specificity Phosphatase 1 in Glucocorticoid-Driven Anti-inflammatory Responses. *Front Immunol.* 2019;10:1446.

55. Moosavi SM, Prabhala P, Ammit AJ. Role and regulation of MKP-1 in airway inflammation. *Respir Res.* 2017;18:154.

56. Bhavsar P, Hew M, Khorasani N, et al. Relative

corticosteroid insensitivity of alveolar macrophages in severe asthma compared with non-severe asthma. *Thorax.* 2008;63:784-790.

57. Quante T, Ng YC, Ramsay EE, et al. Corticosteroids reduce IL-6 in ASM cells via up-regulation of MKP-1. *Am J Respir Cell Mol Biol.* 2008;39:208-217.

58. Li F, Zhang M, Hussain F, et al. Inhibition of p38 MAPK-dependent bronchial contraction after ozone by corticosteroids. *Eur Respir J.* 2011;37:933-942.

초록

미세분리기법을 활용한 신장 조직 전사체 프로파일링 연구

박세훈
의과학 전공
의과학과 대학원
서울대학교

미세분리기법을 이용한 신장 세부조직의 전사체 프로파일링은 사구체와 세뇨관에 국한된 병태생리적 변화를 밝힐 수 있는 방법이다. 저자는 RNA-seq 프로파일링을 미세분리기법으로 분리한 신장조직 검체에서 수행하고자 하였다. 본 연구에는 사구체신염 환자들이 포함되었으며 특정 사구체신염 질환의 특징을 보는 접근과 공통적으로 사구체신염 조직에서 나타나는 변화를 보는 접근을 취하였다. IgA 신장염이 가장 흔한 사구체신염으로서의 임상적 중요성이 있으므로 사구체-전사체 프로파일링 분석에서는 IgA 신장염 환자들의 검체를 대상으로 하였다. 세뇨관의 섬유화 및 손상이 공통적으로 사구체신염 환자들에서 나타나는 늦은 단계의 변화이므로 세뇨관-전사체 프로파일링 분석은 다양한 사구체신염 환자들의 검체를 이용하였다.

사구체-전사체 프로파일링에서 신장기능이 보존된 IgA 신장염 환자들의 RNA-seq 결과를 정상 신장피질 조직의 RNA-seq 결과와 비교하였다. 발현양의 차이가 나는 유전자를 확인하고 이를 바탕으로 기전 분석을 시행하였다. 면역조직화학염색기법 및 혈관사이세포를 이용한 실험실적 타당성 평가를 시행하였다. 총 14건의 IgA 신장염 증례와 10건의 대조군 증례를 대상으로 수행한 RNA-seq 분석에서 연구군과 대조군은 주성분 분석에서 잘 분리되었다. 총 2497개의 발현량의 유의한 차이를 보이는 유전자가 확인되었다. 기전분석에서 세포 이동, 단백-소포 운반, 면역 시스템 및 인산화효소 연관 기전들이

IgA 신장염에서 활성화되있었다. 또한 B세포 및 화학신호 전달 등의/기전들이 IgA 신장염에서 그 발현이 증가하였다. 세포 실험에서 Spleen tyrosine kinase (SYK) 유전자가 IgA 신장염에서 발현량이 증가한 것을 확인하였고, 이를 대상으로 시행한 타당성 평가에서 별개의 IgA 신장염 환자에서 SYK 단백 발현이 증가한 것을 확인하였다. 또한 환자로부터 분리된 IgA1 혈청을 혈관사이세포에 처치하였을 때 SYK 발현이 증가하는 것을 확인하였다.

세뇨관 부분 RNA-seq에서는 65명의 사구체신염 환자가 포함되었으며 이는 43명의 IgA 신장염, 3명의 당뇨병성 신증, 3명의 국소분절사구체경화증, 3명의 루푸스 신염, 3명의 막성 신증, 그리고 9명의 미세변화 신증 환자를 포함한다. 추가로 세뇨관을 미세분리기법으로 분리한 22명의 신절제술을 통해 얻은 신장피질 조직 검체가 대조군으로 포함되었다. 본 분석에서 총 3037개의 유전자의 발현량이 유의한 차이를 보였으며, 그 중에 DUSP1 유전자는 질병군에서 공통적으로 매우 낮아진 발현량을 보였다. 이에 실험적 타당성 확인을 수행하여 DUSP1의 과활성화는 면역지표의 경감을 일으키고 DUSP1의 억제는 면역지표의 활성화를 유발함을 확인하였다. 또한 DUSP1을 활성화한 경우 더 적은 면역억제제로도 강력한 면역억제 효과를 얻을 수 있었다.

결론적으로, 사구체와 세뇨관을 미세분리기법으로 분리하여 수행한 사구체신염 증례의 전사체 프로파일링은 병태생리를 반영하는 결과를 가져다주었다. 본 연구에서 밝혀진 바이오마커에 대한 추가적인 연구를 통해 임상적인 활용성과 치료영역에서의 도입 가능성을 확인하고자 하는 노력이 필요하다.